A Molecular Thermodynamic Model of Coacervation in Solutions of Polycations and Oppositely Charged Micelles

Mohsen Ghasemi,^a Sumanth N. Jamadagni, *a Eric S. Johnson,^a Ronald G. Larson *b

^a The Procter & Gamble Company, Mason, Ohio 45040

^b Department of Chemical Engineering, University of Michigan, Ann Arbor, Michigan 48109

*Corresponding authors

Abstract

To guide rational design of personal care formulations, we formulate a molecular thermodynamic model that predicts coacervation from cationic polymers and mixed micelles containing neutral and anionic surfactants and added salt. These coacervates, which form as a result of dilution of conditioning shampoos during use, deposit conditioning agents and other actives to the scalp or skin and also provide lubrication benefits. Our model accounts for mixing entropy, hydrophobic interactions of polycation with water, free energies of bindings of oppositely charged groups to micelles and polycations, and electrostatic interactions that capture connectivity of charged groups on polycation chain and the micelle. The model outputs are the compositions of surfactants, polycation, salt and water in the coacervate and in its co-existing dilute phase, along with the binding fractions and coacervate volume fraction. We study the effects of overall composition (of surfactants, polycation, and added salt), charge fractions on micelles and polycations, and binding free energies on the phase diagram of coacervates. Then, we perform coacervation experiments for three systems: sodium dodecyl sulfate (SDS) – JR30M, sodium methyl cocoyl taurate (Taurate) – JR30M, and sodium lauryl alaninate (Alaninate) - JR30M, where JR30M is cationic derivative of hydroxyethylcellulose (cat-HEC), and rationalize their coacervation data using our model. For comparison with experiment, we also develop a parametrization scheme to obtain the requisite binding energies and Flory-Huggins γ parameter. We find that our model predictions agree reasonably well with the experimental data, and that the sulfate-free surfactants of Taurate and Alaninate display much larger 2phase regions compared to SDS with JR30M.

1 Introduction: coacervation of polycations with mixed-surfactant micelles

Oppositely charged macromolecules and/or colloids, including polymers, surfactant micelles, proteins, particles, etc., can associate and phase separate into a concentrated phase, referred to as coacervate. Owing to their tunability, such coacervates have found technological applications in conditioning shampoos, foods, water treatment, delivery of pharmaceutics such as water-insoluble anti-cancer drugs, transfection of DNA into cells, and formation of polyelectrolyte multilayers (PEMUs) for encapsulation and sensors.

In anionic surfactant-cationic polymer mixtures, if the concentrated phase that forms following phase separation is a hydrated, soft liquid, it is typically referred to as a "coacervate", which usually has a porous mesh-like internal structure. Polymers and micelles with low charge density, and high salt concentrations, can generally lead to "coacervate" formation. However, if the charge densities of polycation and micelles are high, and/or salt concentration is low, a less-hydrated, solid-like, concentrated phase can form, which is referred to as a "precipitate". The "coacervate" and "precipitate" morphologies give rise to quite different tribological properties upon adsorption onto the hair during dilution of shampoo, with "coacervates" giving smooth, and "precipitates" giving sticky wet, hair feels, respectively. In this study, however, since we are dealing with low-charge-density polycations and our experimental concentrated phases are soft liquids, and also since our model does not, in any event, differentiate between a solid and liquid phase, we use the term "coacervate" to refer to the concentrated phase formed as a result of associative phase separation of surfactants and polycations in aqueous solutions.

Here, we study the equilibrium coacervation in bulk solutions containing mixed anionic-neutral surfactants and cationic polymers, which is a vehicle to deliver silicone and other ingredients to the scalp and provide hair conditioning benefits by shampoos. Note that shampoos contain many other ingredients, including perfumes, preservatives, etc., and these can influence coacervation of polycations and mixed surfactant micelles, and we do not consider such ingredients here. Goddard et al. observed that upon dilution of concentrated (or, neat) shampoo during the shampooing process, the solution phase separates, and conditioning agents are delivered to the hair through deposition of coacervate. 13 This process is known as "dilution-deposition" or "dilution-induced coacervation." Later, Picullel and co-workers found that the surface deposition of coacervates is correlated with coacervate formation in bulk.¹⁴ However, due to the wide range of interactions and forces acting on various length scales, there is a lack of theoretical understanding of the phenomenon. This lack of understanding and of predictive capability is now an acute issue, as efforts to formulate with milder, sulfate-free, surfactants and new biodegradable polycations are now of great interest in the personal care and shampoo industry, and past experience is no longer adequate for optimizing compositions of the new formulations. This motivates us to develop a practical, computationally efficient, molecular thermodynamics model for coacervation from surfactants and polycations to help guide rational design of shampoos to achieve desired shampoo conditioning performance.

Although mixing protocols can lead to non-equilibrium complexes of polyelectrolyte and surfactant micelles, ¹⁵ the current study focuses solely on *equilibrium* phase diagrams of coacervates. The contents and

physiochemical condition of the solution, such as the types¹⁶ and concentrations of PEs, surfactants, and salt, 17-20 the hydrophobicity, 1,16,21 mixing stoichiometry, 22 charge density of polycation and anionic surfactant micelles (or polyanion), ^{12,18,23,24} pH, ^{20,25,26} and temperature, can be used to tune entropic and enthalpic factors that drive coacervation. The main driving force for coacervate formation is widely believed to be the entropy gain from release of initially bound counterions/hydration water from oppositely charged macromolecules (here, polycations and anionic surfactant micelles). 27-30 However, additional factors also contribute to coacervation, including combinatorial binding entropy gain, 30,31 electrostatic interactions between oppositely charged macromolecules, 32,33 and polymer hydrophobicity. 21 Hydrophobicity plays a subtle role in coacervation: it can promote or attenuate coacervation depending on the type of coacervation. In polyelectrolyte (PE) - polyelectrolyte (PE) coacervates, higher levels of polyelectrolyte hydrophobicity make coacervation more favorable, and thus resistant to dissolution (by salt/temperature/polyelectrolyte). 21,34 But, in PE-surfactant micelle mixtures, increased polyelectrolyte hydrophobicity tends to weaken coacervation. As in PE-PE coacervates³⁵, an important parameter affecting coacervate phase behavior of PE-micelle coacervates²² is the mixing stoichiometry, defined as the ratio of positive and negative charges (P/N), where P is the number of charged groups on the polycation and N is the number of anionic surfactants in the micelle (or polyanions for PE-PE coacervates). Near 1:1 charge ratio (i.e., $P \approx N$), coacervation can occur as shown by previous studies.²²

Systematic studies of polycation-surfactant coacervates are rare in the literature, and usually use only sodium lauryl (or laureth) sulfate as the anionic surfactant. Miyake and Kakizawa^{12,18} investigated the effects of added salt, concentration of anionic surfactant, mole ratio of anionic surfactants in the mixed micelles, and charge fraction of polycation in coacervates from cationic hydroxyethylcellulose (cat-HEC) and mixed surfactant lauryl ether sulfate (LES)/ lauroyl amidopropyl betaine (LPB) (see Figure 1). They found that the addition of high enough Na₂SO₄ salt to the solution dissolves the coacervate (Figure 1),^{12,18} in agreement with some previous works.^{36,37} Decreasing the micelle surface charge, by reducing the mole ratio of anionic lauryl ether sulfate surfactant, also shrinks the coacervation region as does a decrease of the polycation charge fraction.

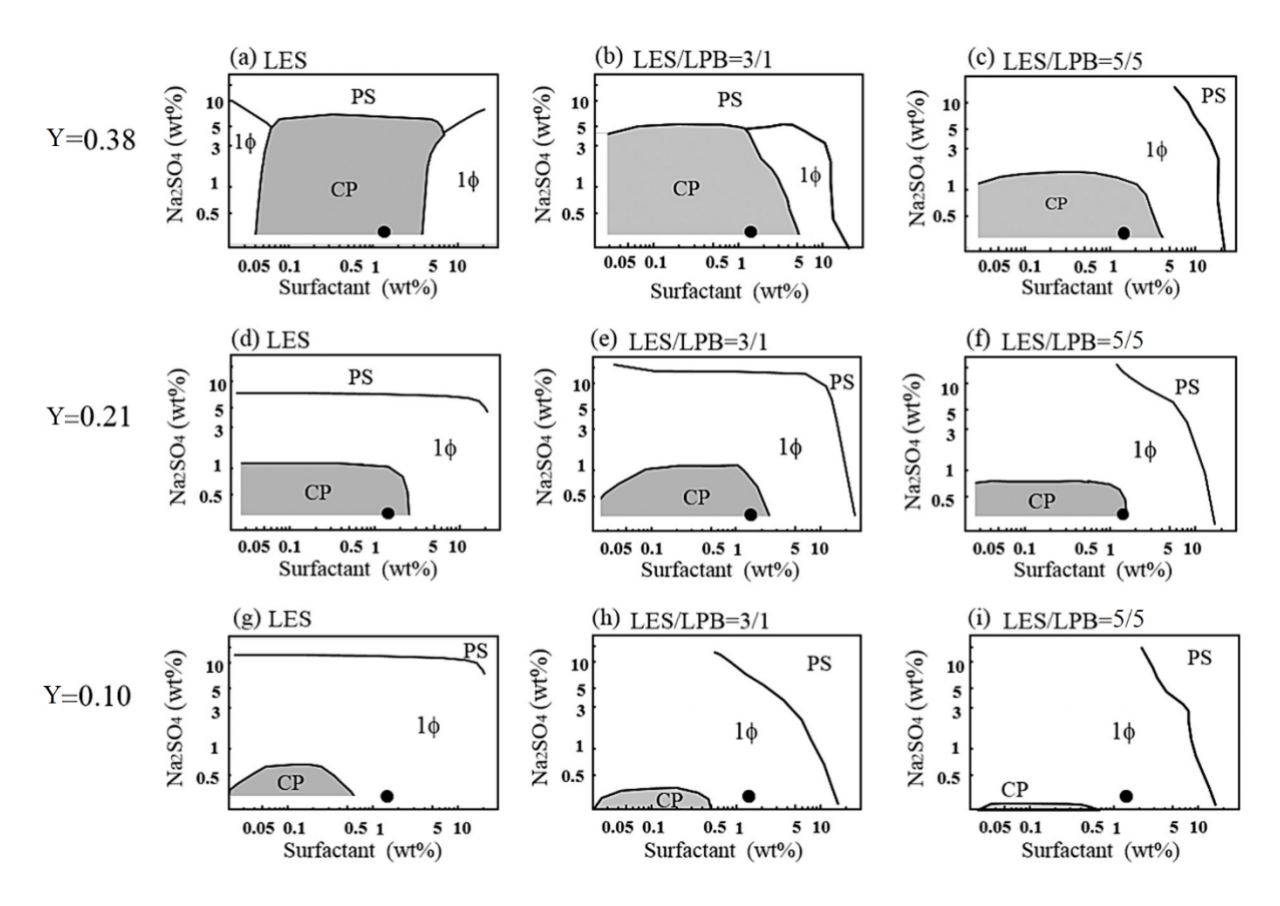


Figure 1. Experimental surfactant/salt phase diagrams of cat-HEC – mixed surfactants (LES/LPB). Here, Y denotes polycation charge fraction and LES/LPB the ratio of ionic/neutral surfactants in the surfactant mixture. The concentration of cat-HEC is fixed at 0.1 wt%. 1 φ , CP, and PS denote the one-phase clear solution, the coacervation region, and a phase separation due to insolubility of species, ¹⁸ respectively. Figure is adapted with permission from Ref 12, Copyright 2023 Advances in Colloid and Interface Science. Note, we believe that the mole fractions of LES/LPB in panels (f) and (i) should be 5/5 (and not 3/1 labeled in Refs 12)

On the theoretical side, Léonforte, Luengo, Guzmán, and co-workers have recently investigated polycation-anionic surfactant complexes in bulk solutions and at negatively-charged silica substrates, mimicking the physico-chemistry of the hair surface, using self-consistent field theory (SCFT)^{38,39} and molecular simulation.⁴⁰ These studies allow one to predict thermodynamic and structural properties, such as the distribution of polymer around surfactant, the hydrodynamic radius of surfactant-polymer aggregates, the thickness and hydration degree of the adsorbed polymer-surfactant layer on the hair-like surfaces, and other properties. Léonforte et al. found that hydrophilic polycations wrap around spherical micelles and bridge between micelles,^{40,41} while highly hydrophobic polycations tend to penetrate inside micelles and transform the micelle structure from spherical to short worm-like micelles.⁴⁰

Allen and Warren developed a cell-based model for adsorption of polymer on micelles and for phase behavior of association of polymer/micelles, where electrostatic interactions were captured using the Poisson-Boltzmann theory. 42,43 They found that polymer bridging between micelles plays an important role in the association of polymers and micelles, 42,43 consistent with the observations of Luengo and coworkers. 40 However, this model is limited to low-charge density polymers and micelles, and it does not

capture ion binding and ion specific effects, making it challenging to be parametrized for different surfactant/polymer chemistries.

Another SCFT-based theoretical model was recently developed by Madinya and Sing for predicting the phase diagram of polycation-micelle coacervation, wherein Monte Carlo simulations were used to determine the surfactant micelle structures and feed those structures into their SCFT.⁴⁴ They found that increasing polycation length and strengthening polycation-surfactant electrostatic energy lead to larger coacervation regions. Shorter polycations have more translational entropy and hence, prefer homogenous solutions and so, disfavor coacervation. However, the effect of polymer length on polycation-surfactant coacervation diminishes for longer polymers, is similar to what is found in polyanion-polycation coacervates. Note that the effect of changes in polymer conformational entropy upon phase separation were ignored in their work as well as in the current study, and only the translational (or, mixing) entropy is considered. The loss of conformational entropy of longer polymers upon complexation is expected to inhibit complexation with micelles and so suppress coacervation.

In this study, we formulate a new molecular thermodynamic model for predicting equilibrium phase behavior of coacervates from polycations and mixed anionic-neutral surfactants derived from our earlier model for polycation-polyanion mixtures. 30,46,47 The model avoids the use of Monte Carlo simulations used by Madinya and Sing, making it simpler, and suitable for practical applications and handling a range of diverse chemistries. Also, our model here extends beyond the limitations of the model of Allen and Warren by considering polymers/micelles of various charge densities, ion binding and ion-specific effects. We perform a parametric study of our model, highlighting important parameters governing coacervation and explaining the observations of Miyake and Kakizawa. Then, we present experimental coacervation phase diagrams for three different surfactants – Alaninate (carboxylate), Taurate (sulfonate) and SDS (sulfate) – with the polycation, JR30M, and show that changing the headgroup chemistry has a dramatic effect of the size of the two-phase region. We then develop a practical parameterization scheme and use that to predict the phase diagrams for the three systems. We find that the model captures the trends in the experimental data and effect of different chemistries quite well. Throughout this work, we also find striking similarities between the behaviors of polycation-polyanion and polycation-surfactant micelle coacervates.

2 Materials and Experimental Methods

2.1 Materials preparation

Polymer JR30M was supplied by Amerchol Inc. (Dow Personal Care) in powder form (i.e., 100% active). JR30M is an amphiphilic, cationic derivative of hydroxyethylcellulose (cat-HEC). The polymer has a charge fraction (defined as the ratio of charged ammonium groups and glucose groups on the main chain) of Y = 0.35, a polymer molecular weight of 2,000,000 Da, and a charge equivalence of 1.3 milli-mole of q/gr of polymer, where "q" is the moles of charges. (We will also compare our theory to experimental data from the literature that involve another grade of cat-HEC, namely "JR400," which, like JR30M, is a cationic hydroxyethylcellulose (cat-HEC), but the JR400 has a molecular weight of 400 kDa rather than 2000 kDa for JR30M.) We consider the coacervation of JR30M and JR400 with sodium dodecyl sulfate (SDS), a sulfate-based, anionic surfactant, was supplied from MP Biomedicals, LLC, in powder form. In our

experiments, we also form coacervates of JR30M with sodium methyl cocoyl taurate (Taurate), a sulfonate-based, anionic surfactant, was supplied by Innospec Inc. as a 32 wt% surfactant solution. We also use sodium cocoyl alaninate (Alaninate) is a titrable, carboxylic-acid-based surfactant and was supplied by Sino Lion USA as a 27.5 wt% surfactant solution.

Stock solutions of each component at various concentrations were prepared by slowly mixing a desired amount of the component in purified water to achieve a target stock solution concentration, and then stirring at 1300 RPM for 1 hour. Preparing highly concentrated, homogenous JR30M solutions (say, > 1.2 wt% polymer) needed special treatment, as one would get tiny flocs upon adding the polymer into water, indicating un-dissolved polymers in the solution. So, JR30M (and also Taurate) stock solutions were heated to 40-45 °C for at least 2 hours to ensure complete dissolution of the polymer. For phase behavior study of titrable Alaninate and JR30M, the pH of the stock solution was adjusted to pH of 7.0 using dilute NaOH or HCl solutions to ensure that the pH was well above the pKa of Alaninate.

2.1 Coacervation experiments

The phase behavior of each pair of polycation and anionic surfactant was measured by simultaneously mixing JR30M and surfactant at different concentrations (or activities) in 20 ml vials. Each vial was stirred using a small magnetic stir-bar and then put in an oven at 40 °C for 48 hours to ensure removal of kinetic traps and attainment of equilibrium. Visual inspection was used to identify the formation of coacervate in each vial. Next, the samples were brought to room temperature for 24 hours, and then another round of visual inspection was performed to confirm that equilibrium coacervates had formed.

3 Results

Here, first we present a parametric study of coacervation using our model, and at the end of the Results in Section 3.7, we compare our model predictions against experimental data. Supporting Information - Section A provides the mathematical formulation of the model, which is a modification of our earlier model for oppositely charged polyelectrolytes only. As in the earlier model for polyelectrolytes only, the micellepolyelectrolyte model incorporates various physiochemical effects in coacervation - mixing and combinatorial binding entropies, Flory-Huggins interactions, binding of oppositely charged groups on the polyelectolytes and micelles as well as binding of small (salt) ions to each of these, and electrostatic interactions using the Random Phase Approximation (RPA). The RPA accounts for the configuration of the polymer and the effect of the non-uniformity of charge it produces on electrostatic free energy. It therefore extends beyond mean-field theories by using fixed intra-molecular correlations between likecharges on a macromolecule (here, on a polycation or micelle). It has been successfully applied in our recent work⁴⁸ on the prediction of charge regulation in weak polyelectrolyte solutions, where the chain conformation drastically changes the deprotonation curve away from the Henderson-Hasselbalch theory in agreement with experiments. Despite the assumption of a fixed form factor, the use of the RPA has also been validated recently against molecular dynamics simulations of counterion condensation of partially charged polyelectrolytes. 49 The RPA can be easily generalized to describe electrostatic interactions of solutions containing charged macromolecules of arbitrary (although, fixed) structure of charge groups,

making it attractive for modeling polyelectrolyte-micelle interactions.⁵⁰ The main difference in the surfactant-polyelectrolyte model relative to the model for polyelectrolytes only is that a spherical-shell form factor representing the micelle negative charge distribution replaces the random-coil form factor of the polyanion used in the earlier model.⁴⁶ The Supporting Information – Section D describes how the choice of form factor of anionic macromolecules (spherical shell vs Gaussian chain) affects their coacervation with polycations. However, note that, if surfactant-polymer binding strengths are high, the specific form factor will have little effect on coacervation, as shown previously by Friedowitz and Qin for polymer-polymer coacervates.⁵¹ A key part of the new model – the binding of counterions to micelles – is discussed in Supporting Information - Section B of this paper. Further, the explicit ion binding in our model also captures short-range binding effects, including non-linear electrostatics (due to, for example, low dielectric constant near charged groups) and non-electrostatic effects (such as entropy gain from release of hydration waters upon binding, etc). The model of Allen and Warren, ^{42,43} which treats electrostatic interactions with Poisson-Boltzmann theory, is another way to capture electrostatic interactions at all length-scales in a unified manner, which, however, does not include the ion binding and ion specific effects.

In this work, we present coacervate phase diagrams in the two-dimensional polymer-surfactant composition space for simplicity. After imposing charge neutrality, the phase diagram can in principle be represented more properly as a three-dimensional quaternary mixture of neutral components (i.e., polymer + counterions, surfactant + counterions, added salt, and water, a slice of which is the ternary phase diagram in the polymer-surfactant plane. Tie lines in the quaternary diagram do not in general lie within this plane, and hence are not shown. Instead, we simply find the boundaries of the two-phase region within the polymer-surfactant slice of the quaternary diagram. The third dimension of this quaternary diagram is explored by replotting the diagram for different levels of added salt. For a full description of this, see Ilekti et al. ⁵² Phase diagrams in the polymer and surfactant concentration space, however, are practically easy to visualize and useful for guiding formulation development.

3.1 Coacervation – reference case

In this section, we analyze coacervation from polycations and (anionic) surfactants using the reference-case values of parameters listed in Table 1. We assume that free energies of counterion binding to polycations and micelles and of ion-pairing between charged monomers of polycation and anionic surfactants in micelles are similar to the free energy of binding of potassium ion to the anionic carboxylate group of poly(acrylic acid), i.e., $\Delta G \approx -4 \, kT$. Although interactions between neutral (or nonionic) surfactants and polycation could be included in the model, for simplicity it is not considered here. It is assumed that surfactants are present only as spherical micelles and we neglect the presence of surfactant monomers in the solution.

Table 1. Micelle aggregation number $(N_{\rm agg})$, polycation degree of polymerization $(N_{\rm C})$, free energies of small cation-surfactant, small anion-polycation monomer, and surfactant-polycation monomer bindings $(\Delta G_{\rm A+}, \Delta G_{\rm C-}, \Delta G_{\rm ip})$, Flory-Huggins chi parameter (χ) , (mole) fractions of anionic surfactants in micelle (X) and of cationic monomers per PC chain (Y), area per surfactant headgroup (a), surfactant tail carbon number (n_c) , added salt concentration $(C_{\rm salt}^{added})$, overall polycation and surfactant concentrations $(C_{isurf}$ and $C_{ipol})$, and normalized sizes of species (ω_i) .

| $[N_{\text{agg}}, N_{\text{C}}]$ $[\Delta G_{\text{A+}}, \Delta G_{\text{C-}}, \Delta G_{\text{ip}}]$ | χ | [X, Y] | $[a, n_c]$ | Cadded salt | C_{isurf} | C_{ipol} | $[\omega_{A}, \omega_{C}, \omega_{+}, \omega_{-}]$ |
|---|---|--------|------------|-------------|-------------|------------|--|
|---|---|--------|------------|-------------|-------------|------------|--|

| [100, 5000] [-4, -4, -5] k _B T | 0.4 | [1, 0.2] | [60 Å ² , 12] | 0 mM | variable | variable | [23.4, 10, 1, 1] |
|---|-----|----------|--------------------------|------|----------|----------|------------------|
|---|-----|----------|--------------------------|------|----------|----------|------------------|

As polycations in personal and hair care formulations are hydrophilic, we choose the chi parameter between cationic monomers and water to be $\chi=0.4$, which is somewhat less than the value (0.5) needed for a long polymer to phase separate from water. The micelle aggregation number is set to 100, which is typical of spherical micelles, and the degree of polymerization of the polycation is chosen to be 5,000. Polycation used for conditioning in shampoo are typically not fully charged. Here, we set the fraction of polycation monomers that are charged to 0.2, and the fraction of anionic surfactants in the micelle to 1.0 (corresponding to purely anionic micelle), although we consider mixed anionic/neutral surfactant micelles later. In this section, no salt is added to the solution, as we explore this effect separately in the next section. However, the counterions for both the surfactant and polymer are included, and so when charged monomers and surfactants are present in the solution at equal concentration, salt from the counterions is present at that same concentration.

Because typical personal care formulations contain an excess of surfactant relative to polymer, only surfactant concentrations that are higher than that of the polycation are explored here – we mark the left boundary of the compositions considered here by the x = y line (and so, this line is not a phase boundary). Another reason to neglect the region that contains more polycations than surfactants, i.e., x < y region, is that our model assumes that all surfactants are present in the form of micelles, which is not valid at very low surfactant concentrations in this region.

Figure 2 shows compositions of polycations and surfactants investigated in section 3.1. The regions shaded in grey in Figure 2 and other plots show the composition region that we did not explore because of the afore-mentioned reasons. The compositions yielding 2 phases, i.e., coacervate formation, are plotted in filled symbols, and 1-phase compositions in open symbols. We observe that 2-phase compositions occur mainly at low concentrations of surfactants and polycations. This is consistent with dilution-deposition during rinsing of shampoos, which is exploited to condition hair.

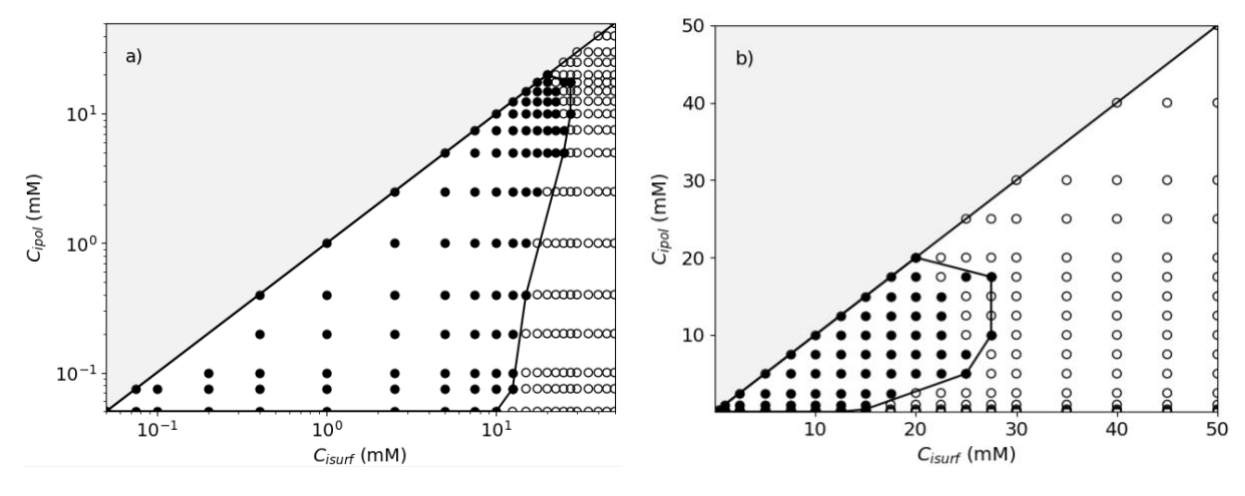
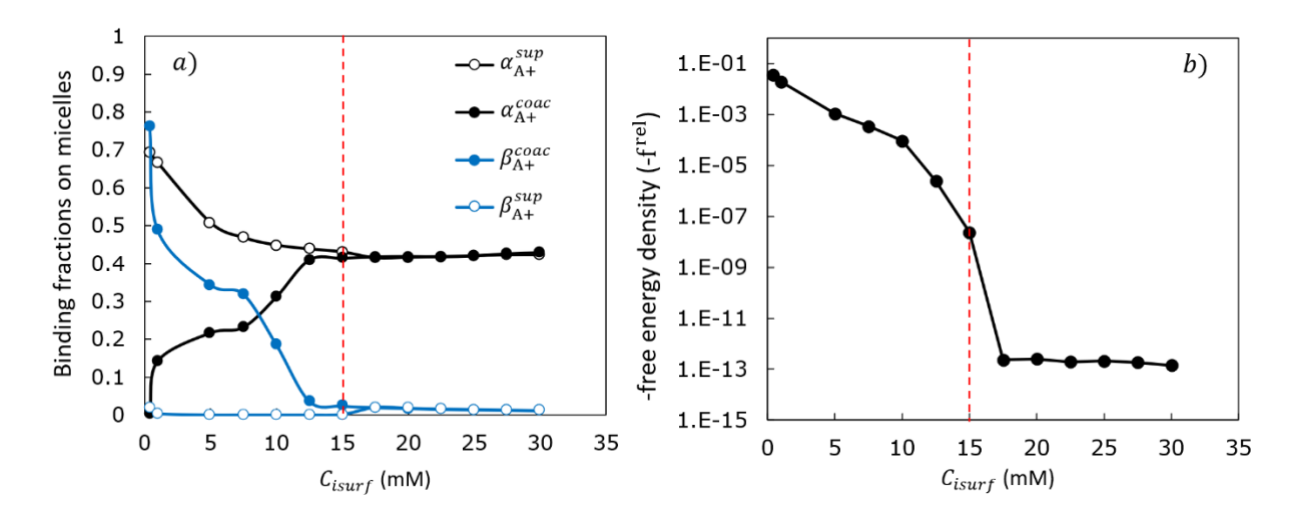


Figure 2. Coacervate phase diagram predicted from our model, which is presented in Supporting Information - Section A. Filled symbols correspond to surfactant-polycation compositions yielding phase separation into coacervate and supernatant phases, and open symbols show the single-phase region. C_{isurf} and C_{ipol} denote the overall concentrations of ionic charges of surfactants and polycation monomers. Both panels are identical except that the

left panel is plotted on logarithmic scale and the right on a linear scale. In this and the following phase diagrams, the diagonal x=y line corresponds to stoichiometric (equimolar) charges on polycations and micelles (i.e., $C_{ipol}=C_{isurf}$), and the line enclosing the filled symbols shows the right boundary of the two-phase region. The lowest C_{ipol} explored in all the parametric studies in this work is $0.05\ mM$.

To explore how coacervation depends on composition, we plot in Figure 3a the fractions of micellar surfactants binding to small-cation (α_{A+}) and to polycation charged monomers (β_A) in the coacervate and supernatant phases as functions of the surfactant concentration at the fixed polycation concentration of $C_{ipol} = 0.4$ mM. At any surfactant concentration lower than (i.e., to the left of) the red, dashed-line, which is the boundary beyond which the solution is single-phase, the small-cation binding fraction α_{A+} on micelles in the supernatant phase is higher than that in the coacervate phase (i.e., $\alpha_{A+}^{coac} < \alpha_{A+}^{sup}$). On the other hand, the fraction of micellar surfactants that bind to polycation charges in the coacervate phase is higher than that in the supernatant phase; i.e., $\beta_A^{coac} > \beta_A^{sup}$ in Figure 3 (note that there is almost no polycation in the supernatant, $\beta_A^{sup} \approx 0$). This indicates that upon mixing of polycations with anionic micelles, the micelles transfer into the coacervate and lose some of their initially bound cations (leading to a decrease in α_{A+}) to complex with polycations (leading to an increase in β_A) and form a coacervate. This directly highlights the role of (mixing) entropy gain in coacervation due to release of initially bound small ions and agrees with the experimental observations of Ilekti et al.⁵² that in forming a complex, sodium polyacrylate (NaPA) displaces the counterions of the surfactant cetyltrimethylammonium bromide (CTABr).



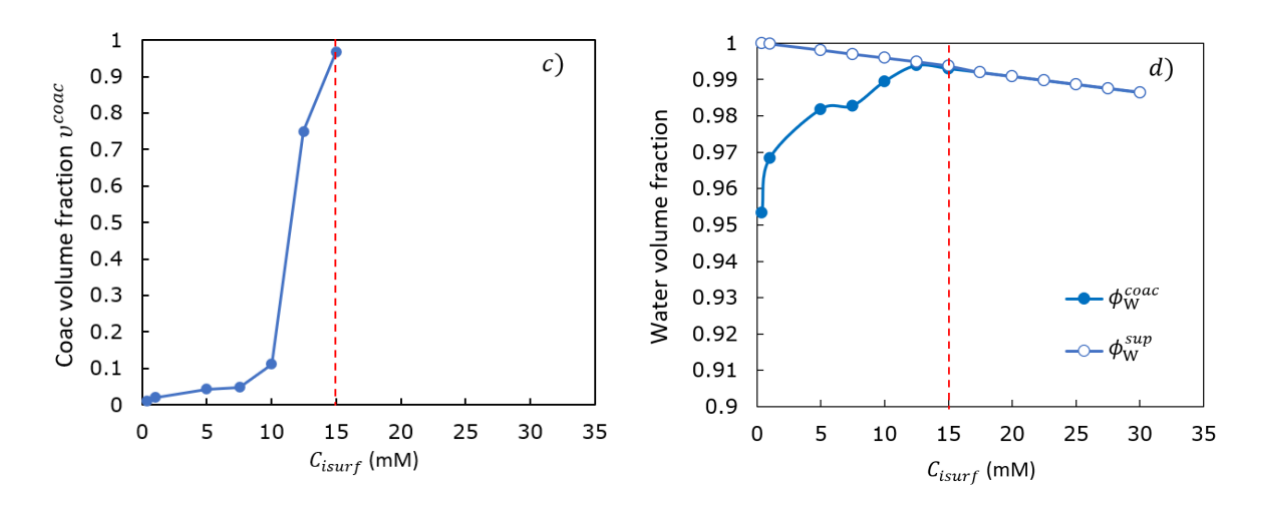


Figure 3. Model predictions for a) binding fractions of small cations (α_{A+} 's) and polycation charges (β_A 's) to anionic surfactants of micelles in the supernatant and coacervate phases, b) negative of the relative free energy density of coacervation $-f^{\rm rel}$, c) coacervate phase volume fraction v^{coac} , and d) volume fraction of water in coacervate ϕ_W^{coac} and in supernatant ϕ_W^{sup} , as functions of overall ionic surfactant concentration C_{isurf} at polycation charged monomer concentration $C_{ipol} = 0.4 \ m{\rm M}$. The red, dashed-line shows the dissolution surfactant concentration, beyond which we enter the one-phase, homogenous region. See Supporting Information - Section A for more details on how the relative free energy density of coacervation is calculated.

At low surfactant concentrations approaching the stoichiometric concentration, which is $C_{isurf} = 0.4 \, m$ M, there is a low concentration of counterions of surfactants and polycations in the solution, namely 0.4 mM. So, release of these initially bound counterions will yield a high entropy gain per ion. (Note that the (mixing) entropy of free ions of type i per unit concentration varies as $\ln(\phi_i)$ with ϕ_i denoting their volume fraction.) Therefore, the relative free energy of coacervation, defined as $f^{rel} = (f^{two \, phase} - f^{one \, phase})/f^{one \, phase}$ with $f^{one \, phase}$ and $f^{two \, phase}$ denoting the free energy densities respectively before and after phase-separation, is more negative, and coacervation is more favorable at more dilute surfactant concentrations; see Figure 3b. Interestingly, besides making coacervation more favorable, decreasing the concentration of surfactant leads to lower coacervate water concentrations (see Figure 3d).

As more surfactant is added into the solution beyond the stoichiometric concentration, some of the additional micelles transfer into the coacervate phase and participate in ion-pairing (or binding) with polycations. The main driving force for this transfer is a gain in combinatorial binding entropy, where a large number of possible binding pairs of opposite charges on, for example, the micelle is more favorable. (In fact, the reason for formation of *macroscopic* coacervates instead of smaller aggregates could be the gain in combinatorial entropy, which favors binding between many different pairs of micelles and polycations.) However, this also leads to high levels of free counterions of micelles in the coacervate, because free counterions of micelles are in equilibrium with the bound ones through the mass action equation (see equation A10 in Supporting Information - Section A). Thus, by adding more surfactant micelles into the solution, some of these will transfer into the coacervate phase, leading to an excess of surfactant over polycation charges. The osmotic pressure of the counterions of the excess surfactants brings water into the coacervate (Figure 3d). High values of water content, such as those in Figure 3d, have been reported for an adsorbed layer of poly(diallyldimethylammonium chloride) (PDADMAC) – sodium laureth sulfate (SLES) on a hair-like surface by Guzmán et al.⁵³ The uptake of excess surfactants by the coacervate

along with the osmotic pressure of the counterions of the excess surfactants increases the coacervate volume fraction; see Figure 3c. This is consistent with a recent study of Schlenoff et al. on non-stoichiometric polyelectrolyte coacervates, where it was observed that as the non-stoichiometry increases, the polymer volume fraction in the coacervate decreases due to an increase in the water content in the coacervate (which results in lower modulus and relaxation time of the coacervate).⁵⁴ Further, in Figure 3c, the shape of the curve of coacervate volume fraction against surfactant concentration (i.e., almost a plateau at low Cisurf followed by a large increase at high C_{isurf}) is reminiscent of that observed in a prior study of coacervation anionic polysaccharide sodium hvaluronate (NaHy) and cationic surfactant tetradecyltrimethylammonium bromide (CTABr).55

The uptake of excess surfactant into the coacervate upon addition of surfactant continues until there is high counterion osmotic pressure in the coacervate and little further entropy gain upon coacervation. At this point ($C_{isurf} \approx 15$ mM), denoted by the red, dashed-line in Figure 3 and referred to as the "dissolution" point, the coacervate is highly hydrated and swollen, with a volume fraction v^{coac} approaching unity. As the dissolution point is approached, the properties of the coacervate and the supernatant, including the water content (Figure 3c) become similar to each other (Figure 3), and the relative free energy of coacervation becomes zero within convergence error (Figure 3b), pointing to loss of driving force for coacervation. The highly water-swollen coacervate near, but not quite at, the dissolution point will likely not scatter light and may not be visible to the naked eye. Thus, it may be difficult to determine experimentally the precise location of the dissolution point.

At this point, it is helpful to clarify some terminology in the 1-phase region. Experimentally as surfactant is added at a fixed polycation concentration and the system changes from a 2-phase composition to a clear, transparent, single-phase system, the coacervate is said to have 'dissolved'. As we explain in the subsequent discussion, it may be more correct to interpret this as the coacervate phase having expanded to a highly hydrated phase with volume fraction of unity due to osmotic driving forces. However, practically, these compositions with a coacervate volume fraction of unity are equivalent to there being no coacervate at all; it is the less water-swollen (and more viscoelastic) coacervates in the 2-phase region that help with product performance (i.e., deposition of colloidal actives and modulation of feel properties.). From that perspective, we refer to the phase boundary in Figure 2 as a "dissolution" boundary, but as explained above, this is dissolution from a practical or visual viewpoint, but not thermodynamic.

Now, we explore the coacervate properties over the entire composition space considered in Figure 2. To do so, we re-plot in Figure 4 the two-phase points from Figure 2, colored according to the values of parameters of interest. The properties of the coacervate at any polycation concentration qualitatively follow a similar patten as presented above at the fixed polycation concentration of $C_{ipol} = 0.4 \, mM$. Consistent with experimental observations, Figure 4 shows that by continuously adding anionic surfactants at any polycation concentration, the coacervate eventually "dissolves" into the supernatant solution, again corroborating the dilution-deposition mechanism of shampoos. Further, we observe that the lowest and most stoichiometric concentrations of polycation and surfactant yield the smallest volumes of coacervate (Figure 4a), the most favorable coacervate formations, as indicated by more negative coacervation free energy f^{rel} (Figure 4b), and the lowest coacervate water contents (not shown). This finding once again confirms the role of entropy gain from releasing initially bound counterions as the driver of coacervation, which is most favorable at the lowest concentrations. Interestingly, Ilekti et al. found that addition of water

to a solution of oppositely charged polymer-surfactant leads to higher concentrations of polymer/surfactant in the coacervate,⁵² yielding a more compact coacervate with a lower water content. This is consistent with our predicted decrease of water concentration in the coacervate at more dilute concentrations of polymer and surfactant (see, for example, Figure 3d; note that the dilution path goes through the origin of composition space.) Further, these results support experimental observations that macroscopic coacervates generally form near a 1:1 charge ratio and at near zero zeta potential.

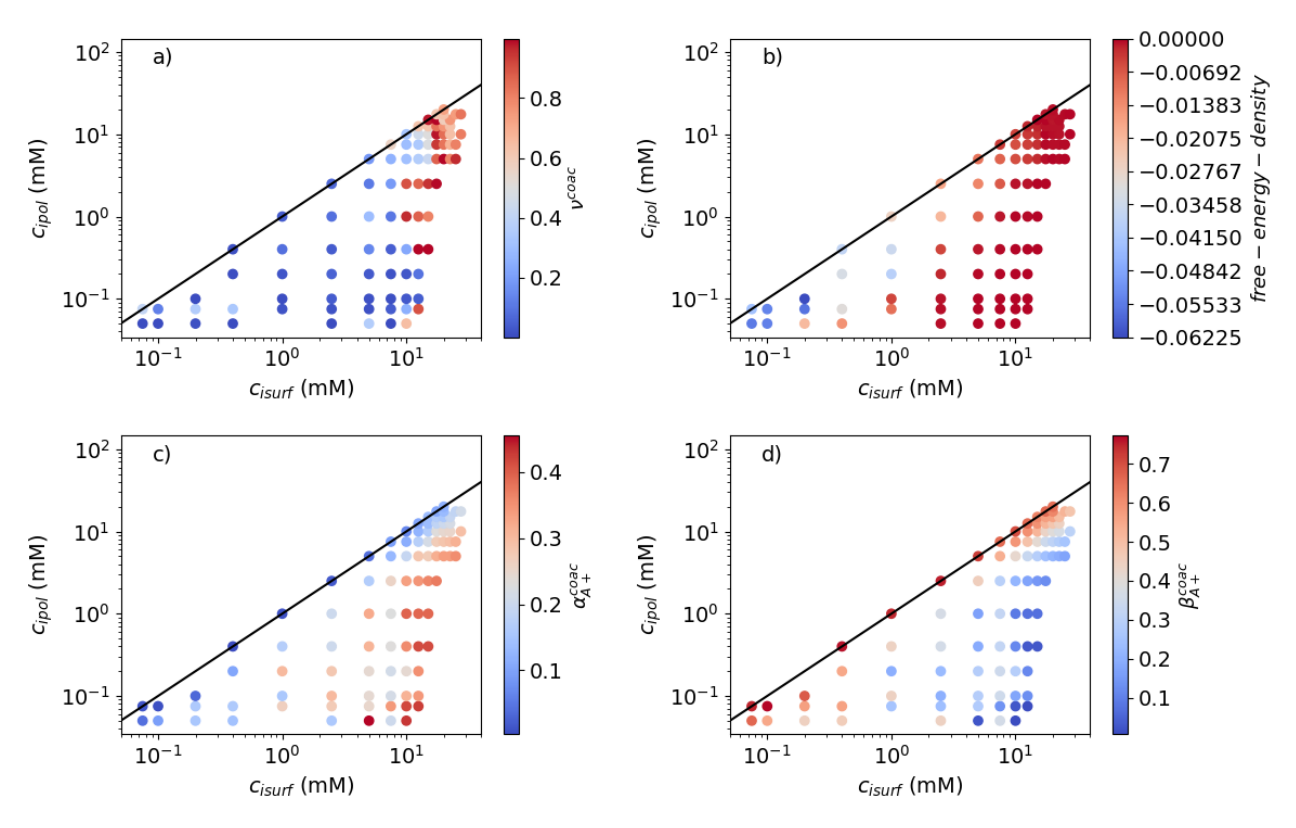


Figure 4. Phase-separated composition points colored by the values of a) coacervate volume fraction ν^{coac} , b) relative free energy density of coacervation f^{rel} , c) binding fraction of small cations (α_{A+}^{coac}) to anionic micelles, and d) binding fraction of polycation charges to anionic micelles (β_A^{coac}) in the coacervate phase.

Note that the solution can transition to a uniform, one-phase, solution even at a 1:1 charge ratio. This is accomplished by addition of large amounts of salt (discussed later) and/or a stoichiometric mixture of a high enough concentration of surfactants and polycations (termed "self-suppression" in the literature), as shown in Figure 2 when these concentrations reach $C_{isurf} = C_{ipol} \approx 20$ mM.

Next, by varying different parameters one at a time, we investigate how coacervation can be tuned by various physiochemical effects.

3.2 Effect of added salt

Salt can either shrink or expand the two-phase region, depending on the concentrations of salt and polymer. Figure 5 shows that the addition of low amounts of salt interestingly enlarges the two-phase region at low polycation concentrations (see green arrow near the bottom in Figure 5b). The expansion of the two-phase

region is due to a "salting-out" effect, where the added salt tends to partition preferentially into the supernatant phase, because the coacervate is already concentrated in the counterions of anionic-surfactants (which are in excess compared to polycations). Hence, the initial partitioning of added ions into the supernatant phase draws in water from the coacervate due to their osmotic pressure, making the coacervate richer in polycation-surfactant and coacervation stronger. This effect has been observed in prior studies of polycation-surfactant coacervates¹⁹ and of polycation-polyanion coacervates,⁴⁷ where in the latter case, it was termed "looping back" of the binodal phase diagram.

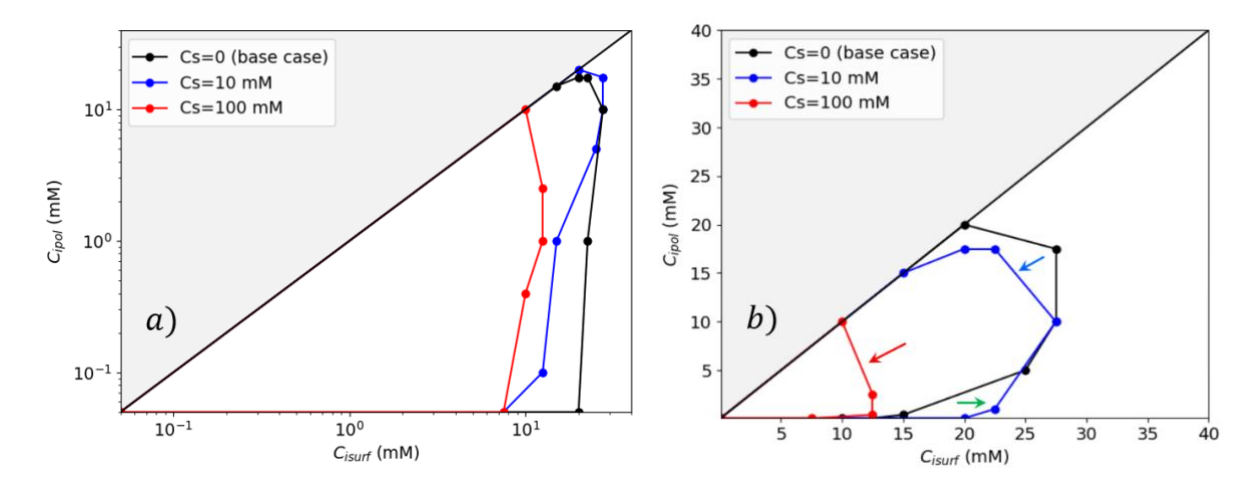


Figure 5. Effect of added salt on the coacervation phase behavior. In this and following figures, both panels are identical except that the left panel is plotted on a logarithmic scale and the right on a linear scale. As discussed in the text, the arrows show the effect of added salt on contraction or expansion of the (right boundary of) the two-phase region compared to the reference case (with no added salt) in different regions of the composition space. The compositions inside the enclosed area correspond to the two-phase region, where both a coacervate and supernatant phase are present.

Partitioning of salt ions into the coacervate becomes appreciable at high salt concentrations, where they break ion-pairs between polycation charged groups and anionic surfactants, leading to shrinkage of coacervation region¹⁹ (overcoming the aforementioned osmotic pressure effects). In Figure 5, we observe that addition of 100 mM of salt significantly shrinks the coacervate phase diagram even at low polymer concentrations (see red arrow on the left in Figure 5b), where the aforementioned osmotic-pressure effects are not present. Also, we note in Figure 5 that near stoichiometric ratios of surfactant to polymer, the two-phase region shrinks immediately with even small amounts of added salt (say, 10 mM; see upper blue arrow in Figure 5b). This is because, in stoichiometric mixtures, the ion concentrations are almost the same in the coacervate and supernatant phases, leading to little osmotic-pressure difference between them. The shrinkage of the two-phase region with added salt has been observed experimentally in cationic hydroxyethylcellulose (cat-HEC) – mixed surfactant lauryl ether sulfate (LES)/ lauroyl amidopropyl betaine (LPB) coacervates (see Figure 1).¹²

It is worth noting that the same effect even drives dissolution of coacervates made from *fixed, stoichiometric* polyanion and polycation concentrations upon doping with salt. Specifically, addition of salt breaks cross-links (or, ion-pairs) between polyanions and polycations, and at high enough added salt this ultimately leads to complete dissolution of the coacervates.^{46,57} A wealth of (experimental, simulation, and

theoretical) polyelectrolyte coacervate studies report phase diagrams in the composition space of salt-polyelectrolyte, where a dome-shaped phase diagram demonstrates the salt doping/screening effect in coacervates at high salt concentrations. ^{21,30,31,57}

3.3 Effect of polycation charge fraction

The polycation charge fraction Y, which is the fraction of monomers that are charged, is an important experimental variable that impacts polycation-surfactant coacervation. As shown in Figure 6, the lower the polycation charge fraction, the smaller the coacervation region. (Note that we here vary the fraction of charged groups on the polycation chain in the model with all other properties of the polycation, including its hydrophobicity, kept fixed. Experimentally, hydrophobicity likely changes along with charge fraction, but we are here examining the effects of each physical property independently.) The shrinkage of the two-phase region upon reducing polymer charge fraction demonstrates that the presence of charges on macromolecules is crucial to produce coacervation, in line with previous studies. 58,59

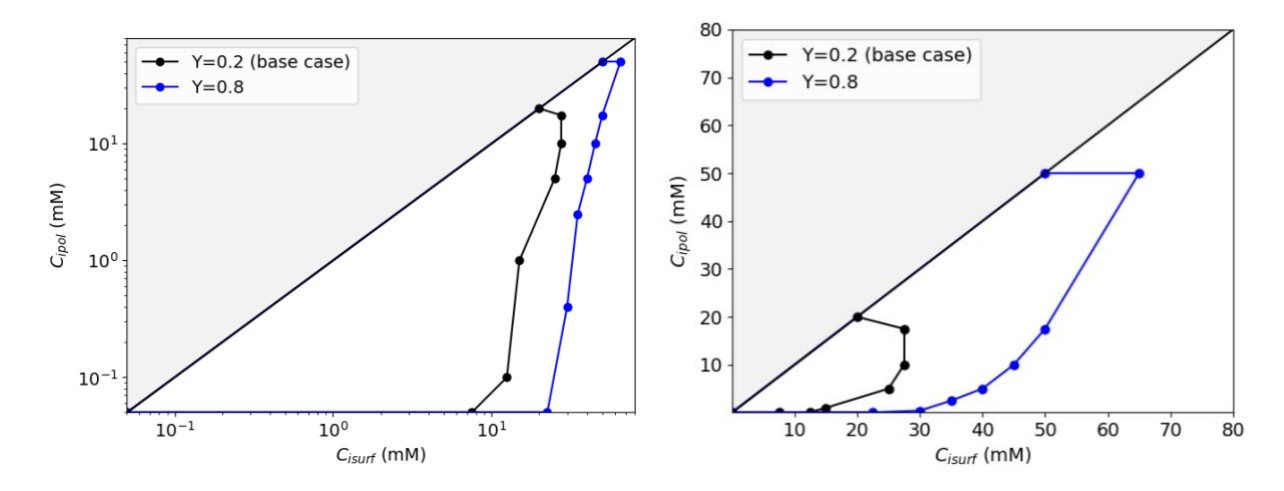


Figure 6. Effect on the phase behavior of coacervate of polycation charge fraction (fraction of monomers charged Y = 0.2 and 0.8).

The fraction of charged monomers *Y* is set by chemistry for strong, pH-insensitive polyelectrolytes, but for weak polyelectrolytes *Y* can be tuned by varying pH. Interestingly, it has been found in experiments that increasing the charge fraction of polyelectrolytes by adjusting pH or by incorporation of more ionic co-monomers improves coacervation of the polyelectrolytes with oppositely charged surfactants, mimicking the predictions in Figure 6. This effect has been observed in a coacervate of poly(4-vinylpyridine N-oxide) (PVPNO) – SDS,²⁵ where the charge density of PVPNO was tuned by pH, in coacervates of sodium poly(acrylate-co-acrylamide) – dodecyltrimethylammonium bromide (DTAB) surfactant⁶⁰ and of poly(acrylate-co-N-isopropylacrylamide) – akyltrimethylammonium acetate surfactant,⁶¹ where in the latter two studies the charge density of each polymer was tuned by the fraction of anionic PA⁻ vs the neutral co monomers of the polymer. Also, Figure 1 shows a similar expansion of the two-phase region with increasing polycation charge fraction in cat-HEC – mixed surfactant (LES/LPB) coacervates.¹²

One might be interested to see how the addition of salt, which mainly attenuates coacervation, and increase of polycation charge density, which promotes coacervation, counter-act each other and affect

coacervation. This was studied by Dubin and co-workers for the linear poly(ethyleneimine) (LPEI) – mixed surfactant triton X-100 (TX100)/SDS mixture at different added salt concentrations and charge fractions of LPEI (tuned by pH.)²⁰ They found that for a given salt concentration, there exists a "critical" polycation charge density above which coacervate can form. Interestingly, Figure 7 shows, similar to their study,²⁰ the existence of critical polycation charge density for coacervation in the presence of salt. In Figure 7, similar to Figure 2, the filled symbols represent coacervate formation, while the open ones show single, homogenous solution. (Note that, the added salt partitions between the co-existing phases of coacervate and supernatant for the filled symbols.)

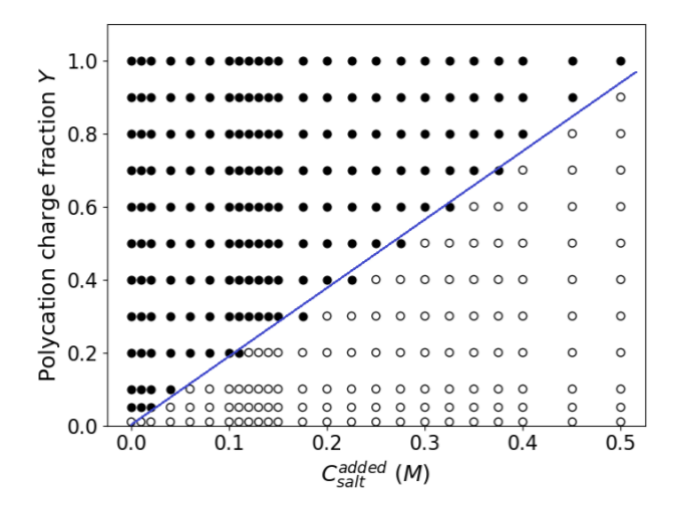


Figure 7. Coacervation phase diagram for solutions containing $C_{isurf}=10$ mM and $C_{ipol}=5.0~Y$ mM at different polycation charge fractions Y and salt concentrations, C_{salt}^{added} . The overall surfactant concentration $C_{isurf}=10$ mM and the maximum overall polycation charged monomer concentration of $C_{ipol}=5.0$ mM were arbitrarily chosen. The blue solid line approximates the border between the two-phase region (i.e., coacervation region, filled symbols) and the one-phase region (open symbols).

3.4 Effect of mole fraction of (an)ionic surfactant in mixed micelles

The mole fraction *X* of (an)ionic surfactant in a mixture with neutral surfactant is a key experimental parameter in designing cleansing formulations, and in this section, we aim at understanding its role in coacervation with polycations. Given the scarcity of systematic experimental data of coacervation phase diagrams on the role of mole fraction of ionic surfactants, here we first explore the predictions of the model (outlined in Supporting Information - Section B) for the binding fraction of counterion on mixed micelles in surfactant solutions, and the use the results to rationalize phase diagrams predicted from our coacervate model for different mole ratios of ionic surfactants.

Figure 8 shows the degree of counterion binding to a mixed micelle composed of cationic surfactant, hexadecylpyridinium chloride monohydrate (CPC), and neutral surfactant, nonylphenol poly-(ethoxylate) (NP(EO)₁₀). As more cationic surfactants are incorporated into the micelle (i.e., increasing X), the counterion binding fraction on the micelle also increases. This is due to higher electrostatic repulsions between cationic surfactants as their numbers increase in the micelles, requiring more bound counterions to relieve these repulsions. One can get a good fit of the model predictions to experimental data of mixed

CPC/NP(EO)₁₀ micelles using the binding strength ($\Delta G_{\rm surf-counterion}$) as the only fitting parameter. (Within our model, the mole fraction of (an)ionic surfactant of micelles, X, is a "quenched" variable, in that micelles always carry the fraction X of (an)ionic surfactants, regardless of the phase into which they partition.)

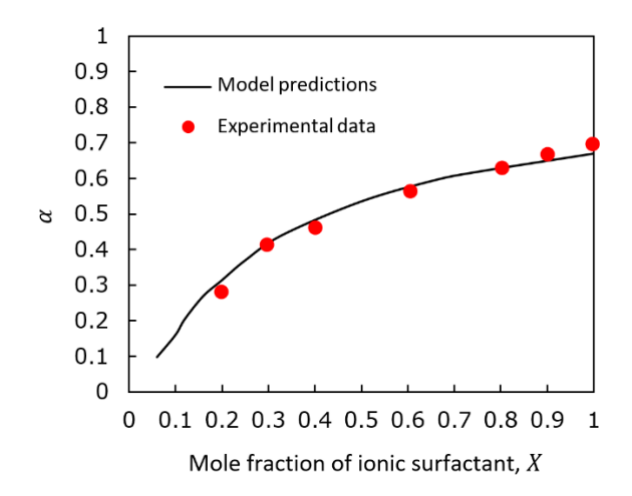


Figure 8. Degree of counterion binding (α) to mixed micelles as a function of the ionic surfactant mole fraction in the micelles, X, with no added salt. The experimental data are from the experiments of Rathman and Scamehorn for CPC/NP(EO)₁₀ micelles,⁶² containing ionic surfactants of hexadecylpyridinium chloride monohydrate (CPC) and non-ionic surfactants of nonylphenol poly-(ethoxylate) (NP(EO)₁₀). Fitted parameter is $\Delta G_{\rm surf-counterion} = -6~k_{\rm B}T$. Other parameters have their standard values in Table 1.

Note that the micelles are cationic in the experiments of Rathman and Scamehorn. Our model is easily applied to cationic micelles, by simply switching the charge signs of micelles and their counterions. The fitted binding free energy of $\Delta G_{\text{surf-counterion}} = -6 k_B T$ in Figure 8 then corresponds to that of counteranion binding to the cationic micelles. Also, although the micelles in Figure 8 contain mixed cationic/nonionic surfactants, the results can be employed to explain the effect of the mole fraction of anionic surfactants in mixed anionic-nonionic surfactant micelles on coacervation with polycation.

Figure 9 shows the effect of the mole fraction X of anionic surfactant in a mixture with neutral surfactant on coacervation with polycations. As the mole fraction X of anionic surfactant is increased, coacervation is enhanced, in agreement with previous work on linear poly(ethyleneimine) (LPEI) – mixed surfactant (TX100/SDS) and PDADMAC – mixed surfactant (TX100/SDS) coacervates. ^{20,63–65} Also, Figure 1 shows a similar expansion of the two-phase region with increasing mole ratio of anionic surfactant in cat-HEC – mixed surfactant (LES/LPB) coacervates. ¹²

In light of Figure 8 and prior to complexation of micelles with polycation, we expect that as the mole fraction of anionic surfactants in micelles is increased, more counterions will bind to the micelles. However, when mixed with polycations, these counterions can be released from the surface of micelles as polycations complex with the anionic micelles, yielding a higher entropy gain and hence, a larger coacervate two-phase region and a lower coacervate water content for more anionic micelles (with higher mole fraction of anionic surfactants *X*). This supports previous experimental work of Luengo and co-workers on the thickness and hydration level of an adsorbed layer of PDADMAC – mixed surfactant (sodium laurethsulfate (SLES) /natural amphoteric coco betaine (CB)) on a hair-like surface from solution.⁵³ They found that, upon reducing the level of CB in the solution (i.e., increasing mole fraction of anionic surfactant), the thickness

of the adsorbed layer decreased significantly due to loss of hydration of the layer. (Although, the work of Luengo et al. concerns deposition on substrates, this behavior is correlated with coacervation in bulk.)¹⁴

Note that the effect of the charge fraction of spherical micelles on their complexation with polycations in Figure 9 is analogous to the effect of the polycation charge fraction in Figure 6.

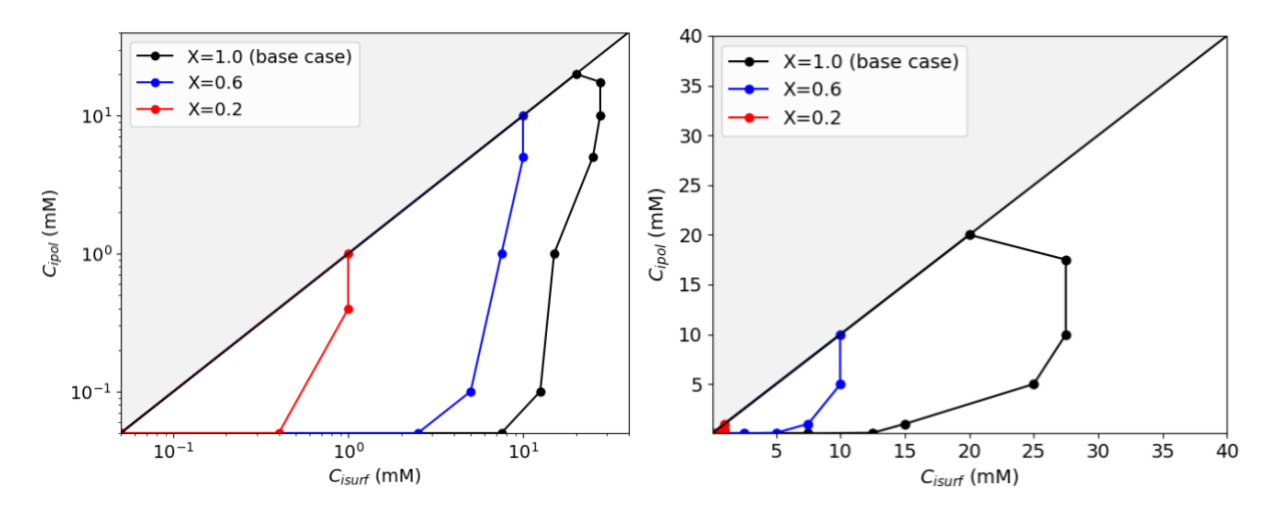


Figure 9. Effect on coacervation of mole fraction of anionic surfactant in the micelle (X = 1.0, 0.6, 0.2).

3.5 Effect of polymer-surfactant ion-pairing strength

The strength of binding between a polycation charged group and the head group of an anionic surfactant, represented by ion-pairing free energy ΔG_{ip} in our model, depends on the type of the binding groups, capturing effects such as electrostatics, hydration shell, and hydrophobicity in their local binding. Figure 10 interestingly shows that stronger ion-pairing between polycation and surfactant yields a smaller two-phase region. To understand this finding, we note that, as discussed before, the coacervate "dissolution" is mainly caused by high osmotic pressure of the counterions of excess micelles in the coacervate (in non-stoichiometric mixtures). So, one can argue that: 1) when ion-pairing is strong, more micelles will partition into the coacervate phase to ion-pair with polycations at fixed overall concentrations, and 2) however, the transfer the micelles is also accompanied by the transfer of their counterions and this will cause osmotic swelling and can dissolve the coacervate. But, when ion-pairing is weak, because micelles hardly partition into coacervate, only addition of high levels of surfactants into the solution can yield the amount of surfactant (and their counterions) in the coacervate required for coacervate dissolution, thereby expanding the coacervation region for weak ion-pairing. Another way to look at this is that strong binding of surfactant to polycation means that this binding can occur at low concentrations of polymer and surfactant, making it easier for it to occur in the single phase, and reducing the driving force for phase separation.

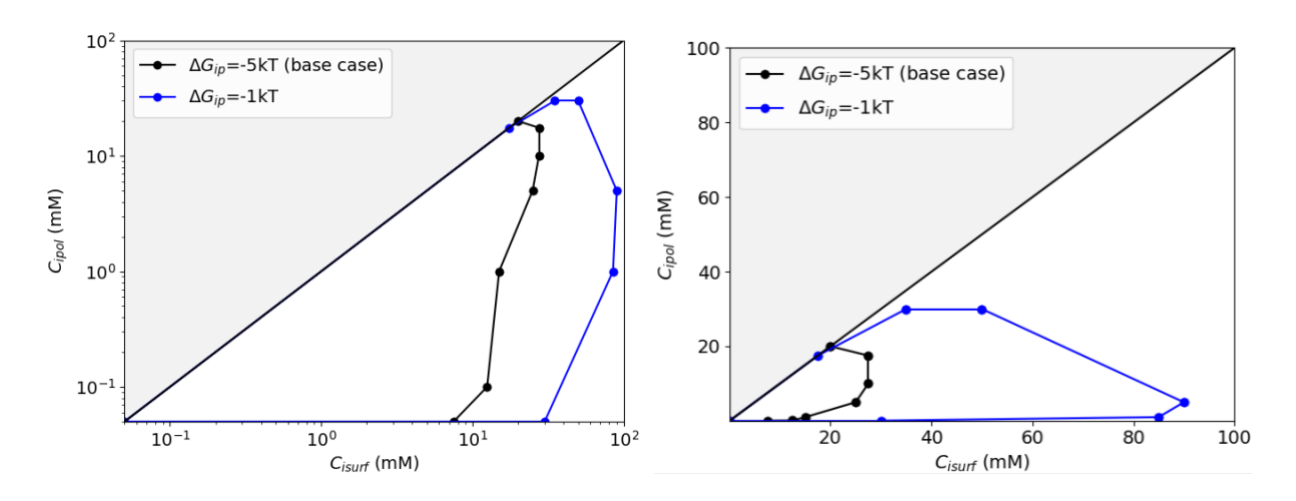


Figure 10. Effect on coacervation phase diagram of the strength of ion-pairing ($\Delta G_{\rm ip} = -5$ vs. $-1~k_{\rm B}T$) between charged groups on the polycation and on the anionic micelle.

3.6 Effect of anionic surfactant-cation binding strength

The degree to which counterions bind to surfactant micelles depends on the headgroup chemistry, salt concentration, and the composition of the micelle in the case of mixed micelles. For example, sodium counterions bind strongly to sodium lauryl sulfate (SLS) and to sodium dodecyl sulfate (SDS) and progressively weakly as ethoxy group are added, as in the ethoxylated SLE1S and SLE2S.⁶⁶ Similarly, counterions bind weakly to surfactants like sodium lauryl methyl taurate^{67,68} or sodium lauryl sarcosinate⁶⁹; this can have important implications for coacervation as described below.

Figure 11 shows that stronger small cation binding to surfactants, ΔG_{A+} , leads to an expansion of the two-phase region at low polycation concentrations, and to a contraction of the two-phase region at high polycation concentrations (say, above 1.0 mM) where the mixture is near stoichiometric in polycation:surfactant charges. The phase diagram expands at low polycation concentration because stronger cation binding to micelles lowers the concentration and osmotic pressure of the free counterions of excess micelles in the coacervate. This then reduces coacervate swelling and pushes the solution farther from one-phase state (i.e., enhances coacervation). Equivalently, when the strength of cation binding to surfactant increases, ion-pairing becomes attenuated, and just as in Figure 10 at low polycation concentrations, the coacervation window in Figure 11 is expanded.

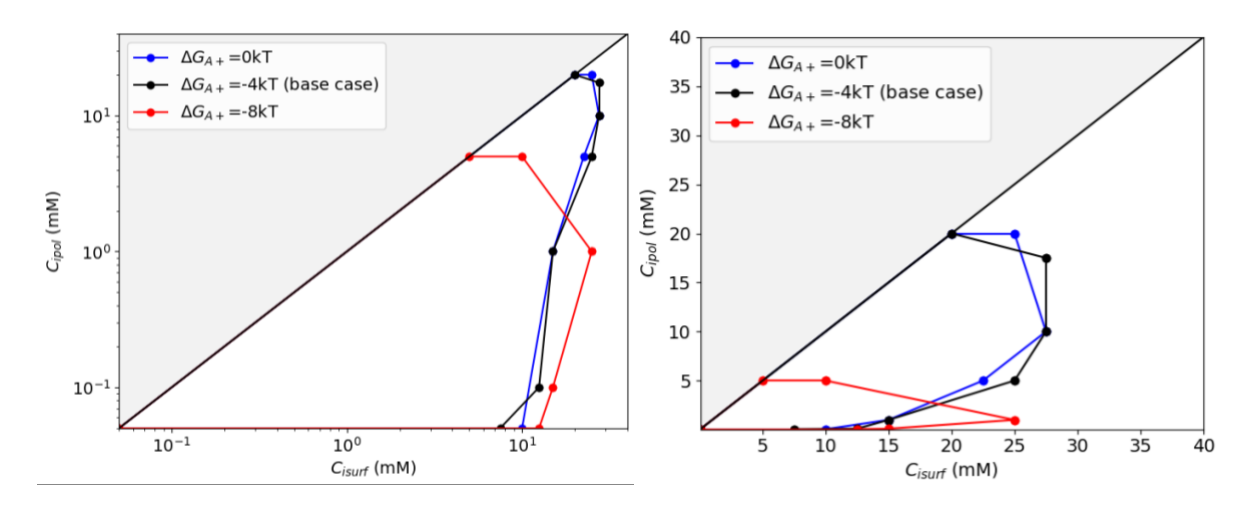


Figure 11. Effect on coacervation phase diagram of surfactant-sodium binding strength ($\Delta G_{A+} = 0$, -4, and $-8 k_B T$).

However, at high polycation concentrations and near stoichiometric mixtures, the aforementioned osmotic-pressure effects are less significant (because there is no excess of micelle charges in the coacervate and small ions are nearly equally partitioned between the coacervate and supernatant). Strengthening cation-surfactant binding then makes the release of counterions (and so, phase separation) less favorable. (Note, the release of initially bound ions is the main driving force for coacervation in stoichiometric mixtures.) Similarly, a number of prior studies show that strongly binding ions easily dissolve stoichiometric polyanion-polycation coacervates through breaking of ion-pairs. 46,70

Note that, a transition of micelle structure from sphere to rod (or cylinder) may occur as the ionsurfactant binding strength is enhanced (for example, along a Hofmeister series for small ion), which can enhance phase separation and coacervation due to lower micelle mixing entropy. We have neglected any change in micelle structure in our model, and we are not interested in varying the type of surfactant counterion.

The response of the coacervation to surfactant-sodium binding strength (i.e., the expansion and the contraction of the two-phase region, depending on polycation concentration) mimics that of added salt in Figure 5.

3.7 Direct comparison of model predictions with experimental data

Sulfate-free surfactants have garnered great commercial interest in the personal care and shampoo industry as they are milder surfactants than current sulfate-based surfactants. Motivated by this goal, we experimentally and theoretically study coacervation phase behavior for three solutions containing polymer JR-30M, a cationic derivative of hydroxyethylcellulose (cat-HEC), and one of the surfactants of sodium dodecyl sulfate (SDS), sodium methyl cocoyl taurate (Taurate), or sodium lauryl alaninate (Alaninate), covering a comparison of sulfate- vs. sulfonate- vs. carboxylate-based surfactant chemistries. We also used data for SDS – JR400 from Ref 17. The polymers JR400 and JR30M are both cat-HEC with the same charge density, and the only difference is that they have molecular weights of 400 kDa and 2000 kDa, respectively.

First, we present experimental data for these mixtures, and then analyze the experimental data using our model. Figure 12 exhibits the experimental coacervate phase diagrams for SDS – JR400, SDS – JR30M,

Taurate – JR30M, and Alaninate – JR30M. The experimental concentrations in Figure 12 range from 4.0 - 0.01 wt% for each surfactant and from 0.6 - 0.01 wt% for the polycation JR30M. For context, a personal care product contains between 12 - 15 wt% surfactant and 0.5 - 1 wt% polymer, and the product is diluted during use. The lines to the left of the solid diagonal line are not of interest here, as these are outside the range of our theory, as explained earlier. For both Taurate and Alaninate, the coacervation region extended up to the highest surfactant and polymer concentrations studied, and hence dashed lines are used in Figure 12 to indicate the minimum extents of these two-phase regions. Only for SDS – JR400 was the complete boundary of the phase diagram with the ranges of concentrations of surfactant and polymer.

Comparison of SDS – JR30M and SDS – JR400 highlights the effect of polycation molecular weight on coacervation. Interestingly, the increase of polymerization degree (or, molecular weight) for JR expands the coacervation region for SDS – JR mixture, especially at high JR concentrations. This is in agreement with prior studies on polycation-surfactant and polycation-polyanion coacervation, where it was found that an increase in chain length leads to expansion of coacervation region due to lower polymer mixing entropy. As Figure 12 shows, changing the type of surfactant has a much more dramatic effect on coacervation than does the polymer molecular weight. The portion of the SDS – JR30M coacervation region (black lines) to the right of the diagonal line is much smaller than that of Taurate – JR30M (red lines, included the dashed portions) or Alaninate – JR30M (blue dashed line); or in other words, when mixed with JR30M, Taurate and Alaninate show much larger two phase regions than does SDS, with the dissolution boundaries of Taurate and Alaninate getting pushed to very high surfactant concentrations. Alaninate – JR30M produced coacervation at all compositions explored in this study, so that the blue dashed line enclosing the Alaninate – JR30M coacervation region is a rectangle that covers the full range of composition examined.

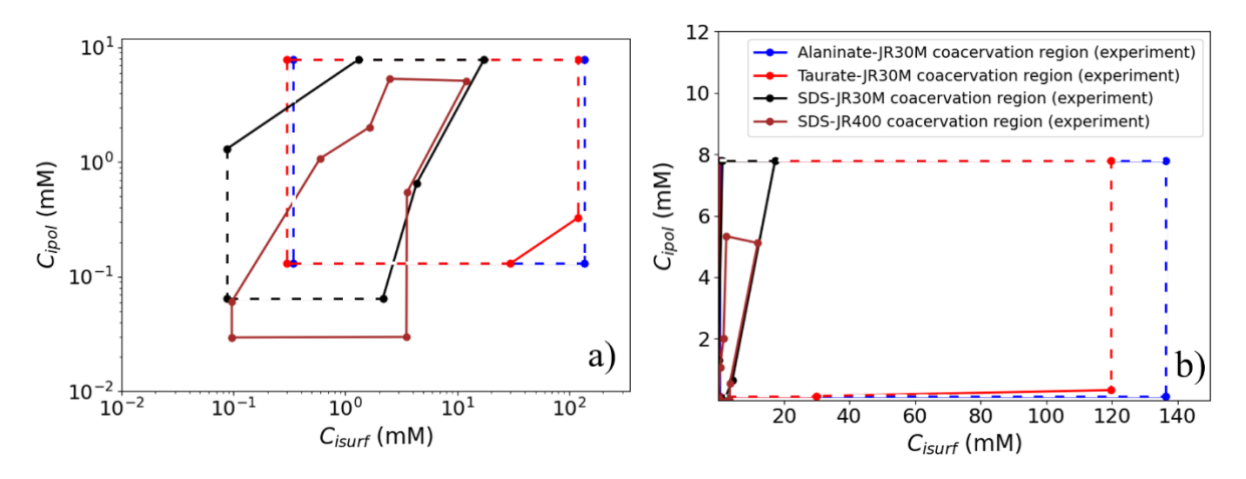


Figure 12. Experimental coacervate phase diagrams for SDS-JR400 (brown), SDS-JR30M (black), Taurate-JR30M (red), and Alaninate-JR30M (blue) on (a) logarithmic and (b) linear scale axes. Dashed lines represent the polymer-surfactant concentration limits explored in the experiments and are lower bounds of the true coacervation boundaries.

Now, we apply the model to the coacervation of SDS – JR400, SDS – JR30M, Taurate – JR30M, and Alaninate – JR30M mixtures. To do so, we first discuss how to obtain the model parameters. The polymer-specific properties, which remain fixed when changing the surfactant type, are listed in Table 2.

Table 2. JR400 and JR30M degrees of polymerization ($N_{\rm C}$), charge fraction of cationic monomers per JR chain Y, small anion-polycation binding free energy ($\Delta G_{\rm C-}$), and polycation monomer-water interaction parameter (χ) for polymer JR.

| $N_{\rm C}({\rm JR400}), N_{\rm C}({\rm JR30M})$ | Y | $\Delta G_{\mathrm{C-}}$ | χ |
|--|------|--------------------------|-------|
| 1000, 5000 | 0.35 | $-4 k_{\mathrm{B}}T$ | -0.63 |

We treat each sugar group on the polymer JR backbone as a monomer. So, the degrees of polymerization of JR400 and JR30M are about 1000 and 5000 (corresponding to MW = 400 kDa and 2000 kDa), respectively. Polymer JR has a charge fraction of Y = 0.35 (For polymer JR, the charge fraction is equal to degree of substitution DS, defined as the fraction of sugar groups carrying a charged quat group, i.e., DS = Y = 0.35). We assume that the free energy of chloride counterion binding to quaternary nitrogen on the polymeris similar in magnitude to that of potassium to poly(acrylic acid), i.e., $\Delta G_{C-} \approx -4 k_B T$. See the Supporting Information – Section D for discussion of the sensitivity of the coacervation region to ΔG_{C-} . We obtained an average value of $\chi = -0.63$ from the COSMOtherm software for the JR monomer-water interaction, consistent with typical hydrophilicity of polycations used in shampoo/body wash formulations. See Supporting Information - Section C for the details of these calculations.

The values of the rest of the model parameters depend on the type of surfactant and its interaction with polymer JR. For simplicity and for all surfactants, we set the carbon tail length to $n_c = 12$, and the area per headgroup to $a = 60 \text{ Å}^2$. Although the exact values of these parameters for SDS, Alaninate, and Taurate may differ slightly from the aforementioned values, for simplicity we keep these values fixed. Micelle aggregation numbers are listed in Table 3.

The last two parameters to be specified are the free energy of the binding of the sodium ion (which is the counterion of all surfactants) to each surfactant, ΔG_{A+} , and the free energy of surfactant – JR binding, ΔG_{ip} . The free energy of sodium binding to each surfactant ΔG_{A+} can be obtained from the study of counterion binding to micelles in surfactant alone solutions. Specifically, we find ΔG_{A+} by matching the predictions from our theory (presented in Supporting Information - Section B) for counterion binding to micelles in surfactant-only solutions to that measured from conductivity experiments; in other words, we feed α_A (taken from conductivity measurements in the literature) into Equation B-1 to extract ΔG_{A+} for binding of sodium to each surfactant micelle. The obtained parameters are shown in Table 3.

Table 3. Aggregation numbers $N_{\rm agg}$ and degrees of counterion dissociation $\alpha_{\rm A}=1-\alpha_{\rm A+}$ of micelles of SDS, Taurate, and Alaninate at their critical micelle concentrations (CMCs) from conductivity measurements. $\Delta G_{\rm A+}$ is the inferred free energy of sodium binding to the micelle obtained from our model in Supporting Information - Section B.

| Surfactant | Surfactant headgroup type | $N_{ m agg}$ | Degree of ionization $lpha_{ m A}$ | $\Delta G_{\mathrm{A+}} \left(k_{\mathrm{B}} T \right)$ |
|------------|---------------------------|--------------------|------------------------------------|--|
| SDS | Sulfate | 6071 | 0.37^{71} | -5.4 |
| Taurate | Sulfonate | 3272 | $0.58^{67,73}$ | -3.45 |
| Alaninate* | Carboxylate | ~ 60 ⁷⁴ | 0.50^{74} | -4.5 |

^{*} For Alaninate, we used literature values of its isomer, Sarcosinate.

The last model parameter, ΔG_{ip} , quantifies the strength of surfactant-polycation pairing and strongly affects coacervation, as shown in Section 3.5, and therefore is a particularly important parameter. Lacking experimental values, we adapt the theory of Li and Wagner, who developed the following empirical expression for the free energy of binding of isolated alkyl surfactants to oppositely charged polymers:⁷⁵

$$\Delta G_{\rm ip} + \ln 55555 \ (mM) = -\ln K (mM^{-1}) = \Delta G_{\rm micellization} - \Delta G_{\rm micellization,SDS} - \ln(A\xi^N)$$

$$= (2 - \alpha_{\rm A}) \ln x_{cmc} - (2 - \alpha_{\rm SDS}) \ln x_{cmc,SDS} - \ln(A\xi^N)$$
(1)

This expression was developed using isothermal titration calorimetry (ITC) data for binding between various surfactants and polycations. One can replace the micellization free energy $\Delta G_{\text{micellization}}$ with $\Delta G_{\text{micellization}} = (2 - \alpha_{\text{A}}) \ln x_{cmc}$ to get the third equality in Equation 1,^{75,76} where the pre-factor $(2 - \alpha_{\text{A}})$ gives the contribution of the bound counterions $(1 - \alpha_{\text{A}})$ plus the aggregated surfactant itself (1) to the micellization free energy, assuming ideal mixing. Here, $\alpha_{\text{A}} = 1 - \alpha_{\text{A+}}$ and x_{cmc} denote the degree of counterion dissociation of the micelle and mole fraction of a surfactant of interest $(x_{cmc} = \frac{\text{CMC}}{55.555})$ at its CMC, respectively. α_{SDS} and $x_{cmc,\text{SDS}}$ are those for a reference case taken to be SDS. A = 50.8 and N = 2.0 are constants obtained by Li and Wagner through fitting of ion-pairing constant to experimental ITC data. The values of α_{A} for SDS, Alaninate, and Taurate at their CMC's are listed in Table 3. Finally, ξ is the reduced linear charge density of polymer ($\xi = l_B/b$ with l_B the Bjerrum length and b the average distance between neighboring charges on the polymer. For the polymer JR, b = 18.69 Å (calculated using ChemDraw 3D) and $\xi = 0.41$.

Using the aforementioned values of ξ and α_A , in Equation 1, we obtain the following ion-pairing free energies: $\Delta G_{\text{SDS-IR}} = -13.1 \, k_{\text{B}}T$, $\Delta G_{\text{Taurate-IR}} = -9.9 \, k_{\text{B}}T$, and $\Delta G_{\text{Alaninate-IR}} = -9.5 \, k_{\text{B}}T$. This indicates that sulfate-containing surfactant SDS binds more strongly to JR than do the carboxylate-based Alaninate surfactant or the sulfonate-based Taurate surfactant. However, the magnitude of these binding free energies are very high for the binding of surfactant headgroups to polycation charged monomers and would lead to unrealistically small coacervation two-phase regions, if used without correction. We note that, the predicted binding free energy from Equation 1 is that of surfactant monomers; we expect a portion of the binding energy of monomers comes from the significant contribution from the hydrophobic interactions of the surfactant tails with the polymer. The binding free energy of micelles, which is the topic of this work, will be much smaller, since the hydrophobic tail of the surfactant is buried in the core of the micelle, and this hydrophobic contribution does not appreciably contribute to the ion-pairing free energy between polymer and micelles. Since most surfactants of interest have the same tail (C_{12}) , all the binding free energies predicted from Equation 1 can be reduced in magnitude by a subtractive constant of about 9.5 $k_{\rm B}T$, obtained by comparison of model predictions with experimental phase diagrams. This estimate is physically reasonable, since the transfer free energy of a methylene group from water into a hydrophobic core is about 1.3 $k_B T_2^{77}$ and association of an alkyl tail of the surfactant with a polymer backbone will not be as favorable as is complete transfer of the tail from an aqueous phase into a hydrocarbon phase. An offset of 9.5 k_BT for a C_{12} tail is $\approx 65\%$ of the free energy change upon complete removal of the tail.

Shifting the values of ion-pairing free energies down by 9.5 k_BT leads to $\Delta G_{SDS-JR} = -3.6 k_BT$, $\Delta G_{Taurate-JR} = -0.4 k_BT$, $\Delta G_{Alaninate-JR} = 0.0 k_BT$. Using these values, the model interestingly predicts

a significant expansion of the coacervation phase diagram for Alaninate – JR30M and Taurate – JR30M compared to that of SDS – JR30M in Figure 13, in rough agreement with the experimental data in Figure 12. In other words, the sulfate-free surfactants of Alaninate and Taurate show a larger two-phase region than does SDS with JR30M. It is also worth noting that this dramatic expansion of the coacervation region occurs with only a few k_BT 's difference in the value of ΔG_{ip} (Also, as indicated by Sections 3.5 and 3.6, we expect that ΔG_{A+} has less effect on the phase diagrams than does ΔG_{ip}).

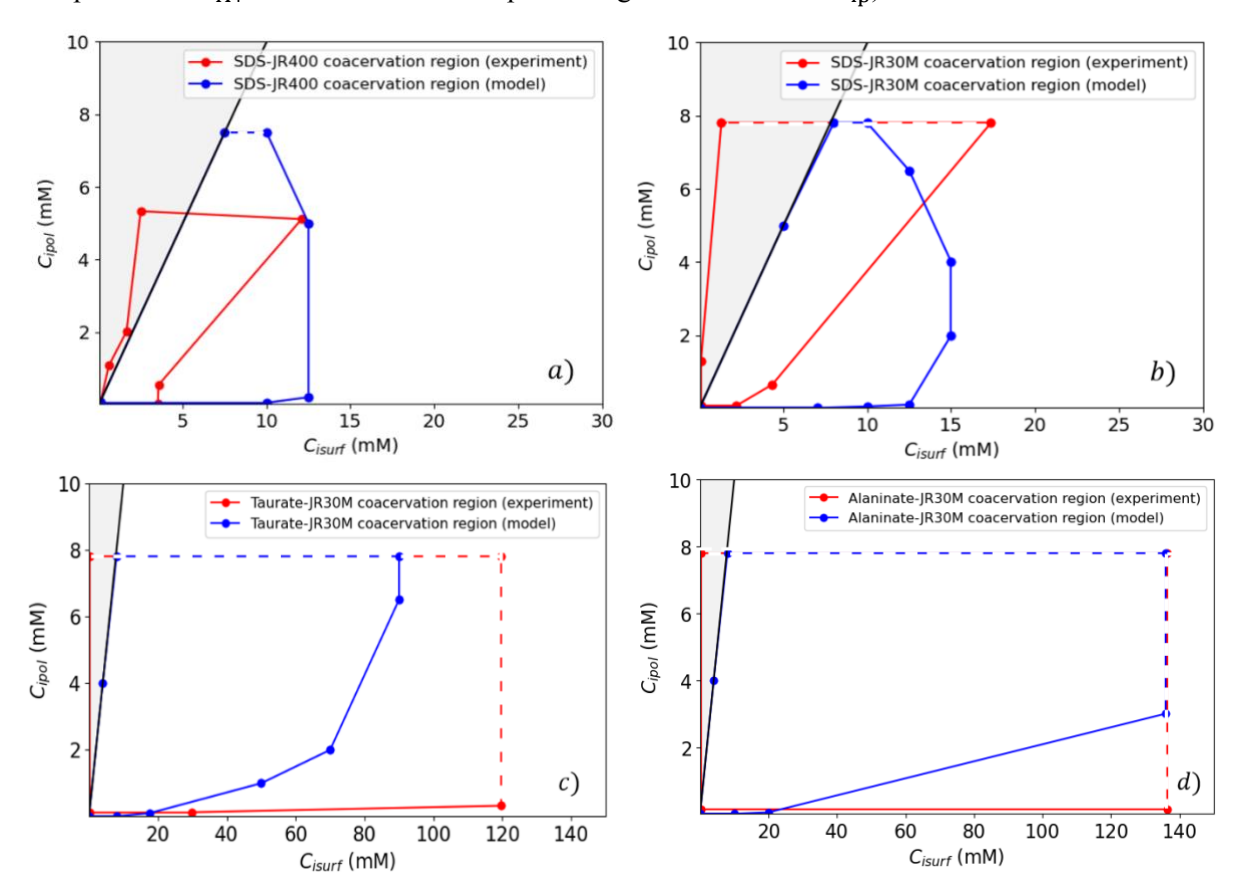


Figure 13. (a) Coacervate phase diagrams of a) SDS-JR400, b) SDS-JR30M, c) Taurate-JR30M, and d) Alaninate-JR30M, predicted from the model (blue) and obtained from experiments (red). Dashed lines represent the polymer-surfactant concentration limits explored here and are not true coacervation boundaries. The experimental phase diagrams here are the same as in Figure 12.

In line with Section 3.5, since SDS binds more strongly to JR30M than do the other surfactants, more micelles and their counterions are partitioned into the coacervate for a given SDS concentration than for the other surfactants, and this leads to a smaller coacervation region for SDS – JR30M, than for Alaninate – JR30M or Taurate – JR30M. As Equation 1 indicates, given the fixed JR charge fraction (Y = 0.35) in these three coacervates, the stronger binding of SDS to JR30M comes from more favorable micellization of the surfactant, i.e., more negative $\Delta G_{\text{micellization,SDS}}$, than for Alaninate or Taurate. However, one may question how the micellization of a surfactant is related to the surfactant binding to polymer. To scrutinize this, one should note that there is a correlation between micellization and aggregation of surfactants on polymers, and perhaps it is actually the formation of aggregates on the polycation that causes the differences observed in the coacervation regions in this study; when a surfactant forms micelles more favorably (i.e.,

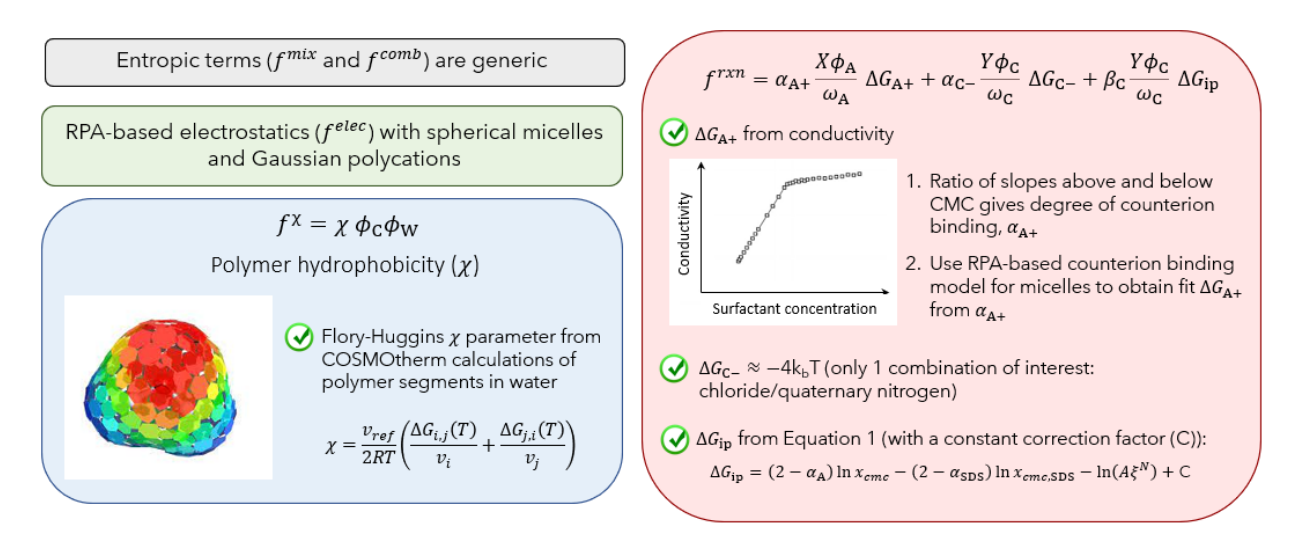
has a more negative micellization free energy $\Delta G_{\text{micellization}}$), it should also favor formation of aggregates on a polymer (i.e., there is an enhanced surfactant-polymer binding), and this can cause a greater uptake of micelles into the coacervate phase and a shrinking of the coacervation region. Note that, these arguments can also explain the observations of Picullel and co-workers, who found that polycations containing more hydrophobic co-monomers, which promote surfactant binding to the polymer, produce smaller coacervations regions than do less hydrophobic polycations.¹

Figure 13 also shows that the predicted coacervation regions of SDS – JR400 and SDS – JR30M are almost the same, with the latter being slightly larger, while the corresponding experimental coacervation regions show greater difference in Figure 12. Nevertheless, the model correctly shows shrinkage of coacervation region as the degree of polymerization of JR is reduced (see Figure SI3 in SI for the case of very short polymer JR).

We summarize our methodology described above for studying coacervation of polycations and anionic micelles in Scheme 1. It shows how our coacervation model parameters can be mapped to specific chemistries of surfactant-polycation mixtures using a combination of simple experimental, simulation, and computational techniques.

Coacervation theoretical framework

$$f = f^{mix} + f^{comb} + f^{elec} + f^{\chi} + f^{rxn}$$



Scheme 1. Methods to estimate the chemistry-specific parameters of the model. The model parameters can be obtained from various methods: i) The Flory-Huggins parameter, χ , can be obtained using COSMOtherm software, ii) the free energy of small cation binding to surfactant, $\Delta G_{\rm A+}$, is accessible through conductivity measurements, iii) one can fix the free energy of small anion binding to polycation, $\Delta G_{\rm C-}$, for fixed polycation/small anion pairs, and iv) the free energy of ion-pairing between surfactant and polycation, $\Delta G_{\rm ip}$, is estimated using a shifted ion-pairing free energy from Equation (1). Other free energy contributions are indirectly dependent on these parameters.

4. Conclusions

We have studied the phase behavior of coacervates formed from polycations and mixed neutral/anionic surfactant micelles using a free energy model adapted from a model of coacervation of polycations and polyanions, by changing the form factor of the polyanion to that of a spherical shell of charges, corresponding to the charge distribution on the surface of a spherical micelle. The model includes the entropy of mixing and combinatorial entropy of binding sequence, electrostatics capturing charge-connectivity effects, and chemical specificities of species through the binding free energies. Further, to enable comparison of theoretical predictions with experiments, we developed a practical parameterization scheme that uses simple computational calculations using COSMOtherm, simple experiments (conductivity), and a previously published correlation in the literature.

Motivated by shift in the personal care industry to milder, sulfate-free surfactants, we experimentally and theoretically study coacervation phase behavior for three solutions containing cationic polymer JR and one of the surfactants of Taurate, Alaninate, or SDS (taken as a reference), covering a comparison of sulfate-vs. sulfonate- vs. carboxylate-based surfactant chemistries. Our model predicts coacervate phase behavior qualitatively similar to that observed experimentally by us, and also that observed for cat-HEC – LES/LPB mixtures by Miyake et. al. In our system, we found that the sulfate-free surfactants studied here show a much larger 2-phase region than SDS with JR30M, and this is primarily due to the weaker binding of these surfactants to the polycation relative to SDS. The coacervation model also predicts enhanced coacervation at low and more stoichiometric concentrations of surfactants and polycations, and hence, further supports the dilution-deposition mechanism for conditioning of shampoos. In addition, a further decrease of the concentrations leads to compaction of coacervate and low coacervate water content, which again explains the frequent experimental observations of more concentrated and compact coacervates upon addition of water to the solution.

Besides the novel experimental data and its explanation using the suitable parameterized models, we presented a number of parametric simulation studies that we briefly summarize here; we found that addition of salt shrinks the two-phase coacervation region almost over the entire composition space; at fixed concentrations of polycation and surfactant, the addition of salt generally dissolves the coacervate through breaking of ion-pairs between polycations and anionic surfactants of micelles, which agrees with previously published experimental data. However, at very low polycation concentrations, addition of low levels of salt interestingly expands the coacervation region, consistent with the "looping back" of the binodal phase diagram of non-stoichiometric mixtures of polyanions and polycations.

When the charge fractions of polycation and/or micelles are increased, larger two-phase coacervation regions are obtained. This supports the notion that the presence of charge on macromolecules is essential to coacervation. Also, our model correctly predicts the existence of critical charge density on polycation for coacervation in the presence of salt and surfactant. We expect a similar prediction (i.e., the existence of critical charge density) for micelles for coacervation from our model. This has been observed in experiments before, where the charge density of micelle is controlled by the mole fraction of ionic surfactants in the micelle.

Further, it is found that stronger ion-pairing between polycation charges and anionic surfactants of micelles shrinks the coacervation region. This effect manifests itself experimentally in the smaller coacervation region of SDS – JR30M, which has strong binding, compared to those of the weakly binding pairs Taurate – JR30M, and Alaninate – JR30M. Finally, the strength of binding of small cations to anionic micelles plays a similar role as that of added salt, with stronger cation-surfactant binding shrinking the coacervation region essentially all over the composition space, except at very low polymer concentrations, where coacervation is enhanced.

This work provides a novel theoretical model for predicting phase behavior of coacervates from polycations and mixed anionic/nonionic surfactants and will be valuable for the development of new personal care formulations with a diverse range of surfactants and cationic polymers. The model can be improved, for example, by using a more accurate empirical expression for ion-pairing into our model or via suitable CAC (critical aggregation concentration) measurements, and by incorporating the effect of unimer (i.e., un-aggregated, monomeric) surfactants, which was ignored in the model presented here. The equilibration between unimers and aggregated surfactants can be important in solutions for which the Critical Micellization Concentration (CMC) of surfactant is high. Furthermore, we assumed that our micelles (or aggregates) are of fixed structure in this work, which can also be relaxed in the future.

Acknowledgements

We thank Xueying Ko (P&G) for help with COSMOtherm calculations and Beth Schubert (P&G) for help with experimental protocols to study coacervation. SNJ thanks Prof. M. Muthukumar for early discussions on this project. RGL acknowledges funding was provided by the National Science Foundation under grants CBET-1907517 and DMR-2100513. Any opinions, findings, and conclusions or recommendations expressed in this material are those of the authors and do not necessarily reflect the views of NSF.

Supporting Information

Model of solution containing polycations, surfactants, salt ions, and water; Model for binding of counterions to micelles in a solution of surfactants, counterions, and water; Details of COSMOtherm simulations to calculate polymer-water interaction parameter χ ; Effects of polycation chain length, of polycation form factor, and of small anion-polycation charge binding strength ΔG_{C-} on coacervation region.

References

- (1) Santos, O.; Johnson, E. S.; Nylander, T.; Panandiker, R. K.; Sivik, M. R.; Piculell, L. Surface Adsorption and Phase Separation of Oppositely Charged Polyion–Surfactant Ion Complexes: 3. Effects of Polyion Hydrophobicity. *Langmuir* **2010**, *26* (12), 9357–9367. https://doi.org/10.1021/la1003353.
- (2) Bouhallab, S.; Croguennec, T. Spontaneous Assembly and Induced Aggregation of Food Proteins. In

- Polyelectrolyte Complexes in the Dispersed and Solid State II: Application Aspects; Müller, M., Ed.; Springer, Berlin, Heidelberg. Berlin, Heidelberg. 2013; pp 67–101.
- (3) Valley, B.; Jing, B.; Ferreira, M.; Zhu, Y. Rapid and Efficient Coacervate Extraction of Cationic Industrial Dyes from Wastewater. *ACS Appl. Mater. Interfaces* **2019**, *11* (7), 7472–7478. https://doi.org/10.1021/acsami.8b21674.
- (4) Barthold, S.; Kletting, S.; Taffner, J.; de Souza Carvalho-Wodarz, C.; Lepeltier, E.; Loretz, B.; Lehr, C.-M. Preparation of Nanosized Coacervates of Positive and Negative Starch Derivatives Intended for Pulmonary Delivery of Proteins. *J. Mater. Chem. B* **2016**, *4* (13), 2377–2386. https://doi.org/10.1039/C6TB00178E.
- (5) Lee, A. L. Z.; Voo, Z. X.; Chin, W.; Ono, R. J.; Yang, C.; Gao, S.; Hedrick, J. L.; Yang, Y. Y. Injectable Coacervate Hydrogel for Delivery of Anticancer Drug-Loaded Nanoparticles in Vivo. *ACS Appl. Mater. Interfaces* **2018**, *10* (16), 13274–13282. https://doi.org/10.1021/acsami.7b14319.
- (6) Felgner, P. L.; Gadek, T. R.; Holm, M.; Roman, R.; Chan, H. W.; Wenz, M.; Northrop, J. P.; Ringold, G. M.; Danielsen, M. Lipofection: A Highly Efficient, Lipid-Mediated DNA-Transfection Procedure. *Proc. Natl. Acad. Sci.* **1987**, *84* (21), 7413–7417. https://doi.org/10.1073/pnas.84.21.7413.
- (7) Correa, S.; Boehnke, N.; Deiss-Yehiely, E.; Hammond, P. T. Solution Conditions Tune and Optimize Loading of Therapeutic Polyelectrolytes into Layer-by-Layer Functionalized Liposomes. *ACS Nano* **2019**, *13* (5), 5623–5634. https://doi.org/10.1021/acsnano.9b00792.
- (8) Alkekhia, D.; Hammond, P. T.; Shukla, A. Layer-by-Layer Biomaterials for Drug Delivery. *Annu. Rev. Biomed. Eng.* **2020**, *22* (1), 1–24. https://doi.org/10.1146/annurev-bioeng-060418-052350.
- (9) Ariga, K.; Hill, J. P.; Ji, Q. Layer-by-Layer Assembly as a Versatile Bottom-up Nanofabrication Technique for Exploratory Research and Realistic Application. *Phys. Chem. Chem. Phys.* **2007**, *9* (19), 2319–2340. https://doi.org/10.1039/B700410A.
- (10) Sukhorukov, G. B.; Donath, E.; Lichtenfeld, H.; Knippel, E.; Knippel, M.; Budde, A.; Möhwald, H. Layer-By-Layer Self Assembly of Polyelectrolytes on Colloidal Particles. *Colloids Surfaces A Physicochem. Eng. Asp.* 1998, 137 (1), 253–266. https://doi.org/https://doi.org/10.1016/S0927-7757(98)00213-1.
- (11) Fares, H. M.; Wang, Q.; Yang, M.; Schlenoff, J. B. Swelling and Inflation in Polyelectrolyte Complexes. *Macromolecules* **2019**, *52* (2), 610–619. https://doi.org/10.1021/acs.macromol.8b01838.
- (12) Miyake, M. Recent Progress of the Characterization of Oppositely Charged Polymer/Surfactant Complex in Dilution Deposition System. *Adv. Colloid Interface Sci.* **2017**, *239*, 146–157. https://doi.org/https://doi.org/10.1016/j.cis.2016.04.007.
- (13) Goddard, E. D.; Gruber, J. V. *Principles of Polymer Science and Technology in Cosmetics and Personal Care*; CRC Press, 1999.
- (14) Svensson, A. V; Huang, L.; Johnson, E. S.; Nylander, T.; Piculell, L. Surface Deposition and Phase Behavior of Oppositely Charged Polyion/Surfactant Ion Complexes. 1. Cationic Guar versus Cationic Hydroxyethylcellulose in Mixtures with Anionic Surfactants. ACS Appl. Mater. Interfaces 2009, 1 (11), 2431– 2442. https://doi.org/10.1021/am900378b.
- (15) Guzmán, E.; Fernández-Peña, L.; Ortega, F.; Rubio, R. G. Equilibrium and Kinetically Trapped Aggregates in Polyelectrolyte–Oppositely Charged Surfactant Mixtures. *Curr. Opin. Colloid Interface Sci.* **2020**, *48*, 91–108. https://doi.org/10.1016/j.cocis.2020.04.002.
- (16) Fu, J.; Fares, H. M.; Schlenoff, J. B. Ion-Pairing Strength in Polyelectrolyte Complexes. *Macromolecules* **2017**, *50*, 1066–1074. https://doi.org/10.1021/acs.macromol.6b02445.
- (17) Li, D.; Kelkar, M. S.; Wagner, N. J. Phase Behavior and Molecular Thermodynamics of Coacervation in Oppositely Charged Polyelectrolyte/Surfactant Systems: A Cationic Polymer JR 400 and Anionic Surfactant

- SDS Mixture. Langmuir 2012, 28 (28), 10348-10362. https://doi.org/10.1021/la301475s.
- (18) Miyake, M.; Kakizawa, Y. Study on the Interaction between Polyelectrolytes and Oppositely Charged Ionic Surfactants. Solubilized State of the Complexes in the Postprecipitation Region. *Colloid Polym. Sci.* **2002**, *280* (1), 18–23. https://doi.org/10.1007/s003960200002.
- (19) Lisa Renee Huisinga. Investigation of the Interactions of Cationic Polyelectrolytes with Anionic Surfactants: Effects of Polymer, Surfactant and Solution Properties, University of Southern Mississippi, 2008.
- (20) Dubin, P. L.; Curran, M. E.; Hua, J. Critical Linear Charge Density for Binding of a Weak Polycation to an Anionic/Nonionic Mixed Micelle. *Langmuir* **1990**, *6* (3), 707–709.
- Li, L.; Rumyantsev, A. M.; Srivastava, S.; Meng, S.; de Pablo, J. J.; Tirrell, M. V. Effect of Solvent Quality on the Phase Behavior of Polyelectrolyte Complexes. *Macromolecules* **2021**, *54* (1), 105–114.
- (22) Hoffmann, I.; Heunemann, P.; Prévost, S.; Schweins, R.; Wagner, N. J.; Gradzielski, M. Self-Aggregation of Mixtures of Oppositely Charged Polyelectrolytes and Surfactants Studied by Rheology, Dynamic Light Scattering and Small-Angle Neutron Scattering. *Langmuir* **2011**, *27* (8), 4386–4396. https://doi.org/10.1021/la104588b.
- Lin, Y.-H.; Song, J.; Forman-Kay, J. D.; Chan, H. S. Random-Phase-Approximation Theory for Sequence-Dependent, Biologically Functional Liquid-Liquid Phase Separation of Intrinsically Disordered Proteins. *J. Mol. Liq.* 2017, 228, 176–193. https://doi.org/https://doi.org/10.1016/j.molliq.2016.09.090.
- (24) Lytle, T. K.; Chang, L.-W.; Markiewicz, N.; Perry, S. L.; Sing, C. E. Designing Electrostatic Interactions via Polyelectrolyte Monomer Sequence. *ACS Cent. Sci.* **2019**, *5* (4), 709–718. https://doi.org/10.1021/acscentsci.9b00087.
- (25) Wang, H.; Fan, Y.; Wang, Y. Thermodynamic Association Behaviors of Sodium Dodecyl Sulfate (SDS) with Poly(4-Vinylpyridine N-Oxide) (PVPNO) at Different PH Values and Ionic Strengths. *J. Surfactants Deterg.* **2017**, *20* (3), 647–657. https://doi.org/https://doi.org/10.1007/s11743-017-1939-7.
- (26) Li, L.; Srivastava, S.; Meng, S.; Ting, J. M.; Tirrell, M. V. Effects of Non-Electrostatic Intermolecular Interactions on the Phase Behavior of PH-Sensitive Polyelectrolyte Complexes. *Macromolecules* **2020**, *53* (18), 7835–7844. https://doi.org/10.1021/acs.macromol.0c00999.
- (27) Gummel, J.; Cousin, F.; Boué, F. Counterions Release from Electrostatic Complexes of Polyelectrolytes and Proteins of Opposite Charge: A Direct Measurement. *J. Am. Chem. Soc.* **2007**, *129* (18), 5806–5807. https://doi.org/10.1021/ja070414t.
- Ou, Z.; Muthukumar, M. Entropy and Enthalpy of Polyelectrolyte Complexation: Langevin Dynamics Simulations. *J. Chem. Phys.* **2006**, *124* (15), 154902. https://doi.org/10.1063/1.2178803.
- (29) Park, S.; Barnes, R.; Lin, Y.; Jeon, B.; Najafi, S.; Delaney, K. T.; Fredrickson, G. H.; Shea, J.-E.; Hwang, D. S.; Han, S. Dehydration Entropy Drives Liquid-Liquid Phase Separation by Molecular Crowding. *Commun. Chem.* **2020**, *3* (1), 83. https://doi.org/10.1038/s42004-020-0328-8.
- (30) Ghasemi, M.; Friedowitz, S.; Larson, R. G. Overcharging of Polyelectrolyte Complexes: An Entropic Phenomenon. *Soft Matter* **2020**, *16*, 10640–10656.
- (31) Lytle, T. K.; Sing, C. E. Transfer Matrix Theory of Polymer Complex Coacervation. *Soft Matter* **2017**, *13* (39), 7001–7012. https://doi.org/10.1039/C7SM01080J.
- (32) Overbeek, J. T. G.; Voorn, M. J. Phase Separation in Polyelectrolyte Solutions. Theory of Complex Coacervation. *J. Cell. Comp. Physiol.* **1957**, *49*, 7–26. https://doi.org/10.1002/jcp.1030490404.
- (33) McCarty, J.; Delaney, K. T.; Danielsen, S. P. O.; Fredrickson, G. H.; Shea, J.-E. Complete Phase Diagram for Liquid–Liquid Phase Separation of Intrinsically Disordered Proteins. *J. Phys. Chem. Lett.* **2019**, *10*, 1644–

1652.

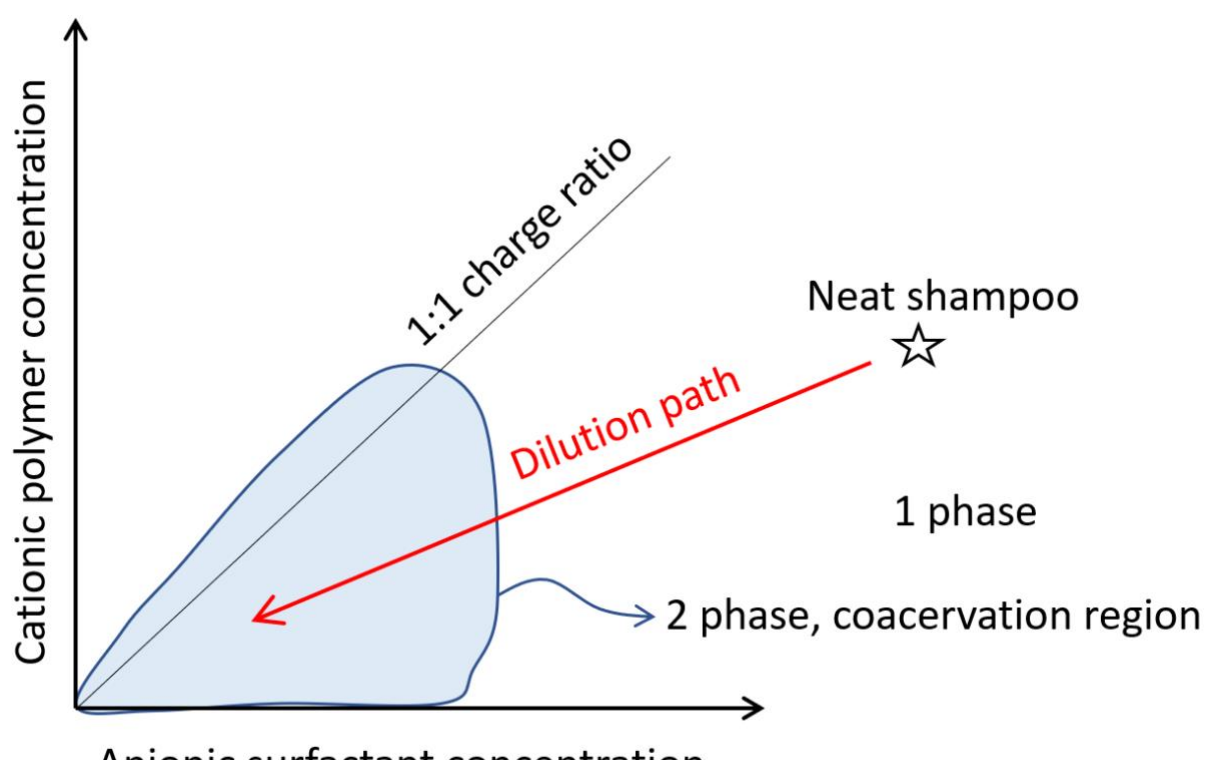
- (34) Gao, J.; Zhan, Q.; Tang, Z.; Huang, Y. The Critical Transition from Soluble Complexes to Colloidal Aggregates of Polyelectrolyte Complexes at Non-Stoichiometric Charge Ratios. *Macromol. Rapid Commun.* **2022**, *43* (7), 2100880. https://doi.org/https://doi.org/10.1002/marc.202100880.
- (35) Kremer, T.; Kovačević, D.; Salopek, J.; Požar, J. Conditions Leading to Polyelectrolyte Complex Overcharging in Solution: Complexation of Poly(Acrylate) Anion with Poly(Allylammonium) Cation. *Macromolecules* **2016**, 49 (22), 8672–8685. https://doi.org/10.1021/acs.macromol.6b01892.
- (36) McQuigg, D. W.; Kaplan, J. I.; Dubin, P. L. Critical Conditions for the Binding of Polyelectrolytes to Small Oppositely Charged Micelles. *J. Phys. Chem.* **1992**, *96* (4), 1973–1978. https://doi.org/10.1021/j100183a080.
- (37) Xia, J.; Zhang, H.; Rigsbee, D. R.; Dubin, P. L.; Shaikh, T. Structural Elucidation of Soluble Polyelectrolyte-Micelle Complexes: Intra- vs Interpolymer Association. *Macromolecules* **1993**, *26* (11), 2759–2766. https://doi.org/10.1021/ma00063a019.
- (38) Guzmán, E.; Fernández-Peña, L.; S Luengo, G.; Rubio, A. M.; Rey, A.; Léonforte, F. Self-Consistent Mean Field Calculations of Polyelectrolyte-Surfactant Mixtures in Solution and upon Adsorption onto Negatively Charged Surfaces. *Polymers (Basel).* **2020**, *12* (3). https://doi.org/10.3390/polym12030624.
- (39) Hernández-Rivas, M.; Guzmán, E.; Fernández-Peña, L.; Akanno, A.; Greaves, A.; Léonforte, F.; Ortega, F.; G. Rubio, R.; Luengo, G. S. Deposition of Synthetic and Bio-Based Polycations onto Negatively Charged Solid Surfaces: Effect of the Polymer Cationicity, Ionic Strength, and the Addition of an Anionic Surfactant. *Colloids and Interfaces*. 2020. https://doi.org/10.3390/colloids4030033.
- (40) Coscia, B. J.; Shelley, J. C.; Browning, A. R.; Sanders, J. M.; Chaudret, R.; Rozot, R.; Léonforte, F.; Halls, M. D.; Luengo, G. S. Shearing Friction Behaviour of Synthetic Polymers Compared to a Functionalized Polysaccharide on Biomimetic Surfaces: Models for the Prediction of Performance of Eco-Designed Formulations. *Phys. Chem. Chem. Phys.* **2023**, *25* (3), 1768–1780. https://doi.org/10.1039/D2CP05465E.
- (41) Banerjee, S.; Cazeneuve, C.; Baghdadli, N.; Ringeissen, S.; Leermakers, F. A. M.; Luengo, G. S. Surfactant–Polymer Interactions: Molecular Architecture Does Matter. *Soft Matter* **2015**, *11* (12), 2504–2511. https://doi.org/10.1039/C5SM00117J.
- (42) Allen, R. J.; Warren, P. B. Complexation and Phase Behavior of Oppositely Charged Polyelectrolyte/Macroion Systems. *Langmuir* **2004**, *20* (5), 1997–2009. https://doi.org/10.1021/la0356553.
- (43) R. J. Allen; P. B. Warren. Phase Behaviour of Oppositely Charged Polymer/Surfactant Mixtures. *Europhys. Lett.* **2003**, *64* (4), 468. https://doi.org/10.1209/epl/i2003-00234-2.
- (44) Madinya, J. J.; Sing, C. E. Hybrid Field Theory and Particle Simulation Model of Polyelectrolyte—Surfactant Coacervation. *Macromolecules* **2022**, *55* (6), 2358–2373. https://doi.org/10.1021/acs.macromol.2c00187.
- (45) Spruijt, E.; Westphal, A. H.; Borst, J. W.; Cohen Stuart, M. A.; van der Gucht, J. Binodal Compositions of Polyelectrolyte Complexes. *Macromolecules* **2010**, *43* (15), 6476–6484. https://doi.org/10.1021/ma101031t.
- (46) Ghasemi, M.; Friedowitz, S.; Larson, R. G. Analysis of Partitioning of Salt Through Doping of Polyelectrolyte Complex Coacervates. *Macromolecules* **2020**, *53* (16), 6928–6945. https://doi.org/10.1021/acs.macromol.0c00797.
- (47) Friedowitz, S.; Lou, J.; Barker, K. P.; Will, K.; Xia, Y.; Qin, J. Looping-in Complexation and Ion Partitioning in Nonstoichiometric Polyelectrolyte Mixtures. *Sci. Adv.* **2021**, *7* (31). https://doi.org/10.1126/sciadv.abg8654.
- (48) Ghasemi, M.; Larson, R. G. Role of Electrostatic Interactions in Charge Regulation of Weakly Dissociating Polyacids. *Prog. Polym. Sci.* **2021**, *112*, 101322. https://doi.org/https://doi.org/10.1016/j.progpolymsci.2020.101322.

- (49) Tian, W.; Ghasemi, M.; Larson, R. G. Extracting Free Energies of Counterion Binding to Polyelectrolytes by Molecular Dynamics Simulations. *J. Chem. Phys.* **2021**, *155*, 114902.
- (50) Qin, J.; de Pablo, J. J. Criticality and Connectivity in Macromolecular Charge Complexation. *Macromolecules* **2016**, *49* (22), 8789–8800. https://doi.org/10.1021/acs.macromol.6b02113.
- (51) Friedowitz, S.; Qin, J. Reversible Ion Binding for Polyelectrolytes with Adaptive Conformations. *AIChE J.* **2021**, *67* (12), e17426.
- (52) Ilekti, P.; Piculell, L.; Tournilhac, F.; Cabane, B. How To Concentrate an Aqueous Polyelectrolyte/Surfactant Mixture by Adding Water. *J. Phys. Chem. B* **1998**, *102* (2), 344–351. https://doi.org/10.1021/jp972575x.
- (53) Guzmán, E.; Llamas, S.; Fernández-Peña, L.; Léonforte, F.; Baghdadli, N.; Cazeneuve, C.; Ortega, F.; Rubio, R. G.; Luengo, G. S. Effect of a Natural Amphoteric Surfactant in the Bulk and Adsorption Behavior of Polyelectrolyte-Surfactant Mixtures. *Colloids Surfaces A Physicochem. Eng. Asp.* 2020, 585, 124178. https://doi.org/https://doi.org/10.1016/j.colsurfa.2019.124178.
- (54) Chen, Y.; Yang, M.; Shaheen, S. A.; Schlenoff, J. B. Influence of Nonstoichiometry on the Viscoelastic Properties of a Polyelectrolyte Complex. *Macromolecules* **2021**, *54* (17), 7890–7899. https://doi.org/10.1021/acs.macromol.1c01154.
- (55) Thalberg, K.; Lindman, B.; Karlstroem, G. Phase Behavior of a System of Cationic Surfactant and Anionic Polyelectrolyte: The Effect of Salt. *J. Phys. Chem.* **1991**, *95* (15), 6004–6011. https://doi.org/10.1021/j100168a053.
- (56) Xu, A. Y.; Kizilay, E.; Madro, S. P.; Vadenais, J. Z.; McDonald, K. W.; Dubin, P. L. Dilution Induced Coacervation in Polyelectrolyte—Micelle and Polyelectrolyte—Protein Systems. *Soft Matter* **2018**, *14* (12), 2391–2399. https://doi.org/10.1039/C7SM02293J.
- (57) Wang, Q.; Schlenoff, J. B. The Polyelectrolyte Complex/Coacervate Continuum. *Macromolecules* **2014**, *47* (9), 3108–3116. https://doi.org/10.1021/ma500500q.
- (58) Wang, Y.; Kimura, K.; Huang, Q.; Dubin, P. L.; Jaeger, W. Effects of Salt on Polyelectrolyte–Micelle Coacervation. *Macromolecules* **1999**, *32* (21), 7128–7134. https://doi.org/10.1021/ma990972v.
- (59) Burgess, D. J. Practical Analysis of Complex Coacervate Systems. *J. Colloid Interface Sci.* **1990**, *140* (1), 227–238. https://doi.org/https://doi.org/10.1016/0021-9797(90)90338-O.
- (60) Ranganathan, S.; Kwak, J. C. T. Effect of Polymer Charge Density on the Phase Behavior of Sodium Poly(Acrylate-Co-Acrylamide)–DTAB Systems. *Langmuir* **1996**, *12* (5), 1381–1390. https://doi.org/10.1021/la950387x.
- (61) dos Santos, S.; Gustavsson, C.; Gudmundsson, C.; Linse, P.; Piculell, L. When Do Water-Insoluble Polyion–Surfactant Ion Complex Salts "Redissolve" by Added Excess Surfactant? *Langmuir* **2011**, *27* (2), 592–603. https://doi.org/10.1021/la104256g.
- (62) Rathman, J. F.; Scamehorn, J. F. Counterion Binding on Mixed Micelles. *J. Phys. Chem.* **1984**, *88* (24), 5807–5816. https://doi.org/10.1021/j150668a014.
- (63) Li, Y.; Dubin, P. L.; Havel, H. A.; Edwards, S. L.; Dautzenberg, H. Complex Formation between Polyelectrolyte and Oppositely Charged Mixed Micelles: Soluble Complexes vs Coacervation. *Langmuir* **1995**, *11* (7), 2486–2492. https://doi.org/10.1021/la00007a029.
- (64) Khan, N.; Brettmann, B. Intermolecular Interactions in Polyelectrolyte and Surfactant Complexes in Solution. *Polymers* . 2019. https://doi.org/10.3390/polym11010051.
- (65) Wang, Y.; Kimura, K.; Dubin, P. L.; Jaeger, W. Polyelectrolyte–Micelle Coacervation: Effects of Micelle Surface Charge Density, Polymer Molecular Weight, and Polymer/Surfactant Ratio. *Macromolecules* **2000**,

- 33 (9), 3324–3331. https://doi.org/10.1021/ma991886y.
- (66) Barry, B. W.; Wilson, R. C. M. C., Counterion Binding and Thermodynamics of Ethoxylated Anionic and Cationic Surfactants. *Colloid Polym. Sci.* **1978**, *256* (3), 251–260. https://doi.org/10.1007/BF01550555.
- (67) Kim, J.-H.; Kim, T.-Y.; Ju, M.-J.; Nam, K.-D. Studies on the Surfactants of the N-Acyl Amino Acid(Part 9) -The Effect of Temperature and Electrolytes on the Micellization of Sodium N-Lauroyl-N-Methyl-Taurate-. *Appl. Chem. Eng.* **1996**, *7* (3), 401–409.
- (68) Ray, G. B.; Ghosh, S.; Moulik, S. P. Physicochemical Studies on the Interfacial and Bulk Behaviors of Sodium N-Dodecanoyl Sarcosinate (SDDS). *J. Surfactants Deterg.* **2009**, *12* (2), 131–143. https://doi.org/https://doi.org/10.1007/s11743-008-1105-3.
- (69) Bordes, R.; Tropsch, J.; Holmberg, K. Role of an Amide Bond for Self-Assembly of Surfactants. *Langmuir* **2010**, *26* (5), 3077–3083. https://doi.org/10.1021/la902979m.
- (70) Ghostine, R. A.; Shamoun, R. F.; Schlenoff, J. B. Doping and Diffusion in an Extruded Saloplastic Polyelectrolyte Complex. *Macromolecules* **2013**, *46* (10), 4089–4094.
- (71) Thévenot, C.; Grassl, B.; Bastiat, G.; Binana, W. Aggregation Number and Critical Micellar Concentration of Surfactant Determined by Time-Dependent Static Light Scattering (TDSLS) and Conductivity. *Colloids Surfaces A Physicochem. Eng. Asp.* 2005, 252 (2), 105–111. https://doi.org/https://doi.org/10.1016/j.colsurfa.2004.10.062.
- (72) Miyazawa, Kiyoshi Takahashi, Toshinobu, Kohashi, H.; Ishida, M.; Yoshino, S.; Kamogawa, K.; Sakai, H.; Abe, M. Stepwise Changes in Solution Properties of N-Lauroyl-n-Methyltaurinates Having Na⁺, Mg2+, and Ca2+ as Counter Ions: Successive Micellar Reorganization in Relation to Binding of Counter Ions: Successive Micellar Reorganization in Rela. *J. Japan Oil Chem. Soc.* **1998**, *47* (6), 563–576.
- (73) Tsubone, K.; Rosen, M. J. Structural Effect on Surface Activities of Anionic Surfactants Having N-Acyl-N-Methylamide and Carboxylate Groups. *J. Colloid Interface Sci.* **2001**, *244* (2), 394–398. https://doi.org/10.1006/jcis.2001.7995.
- (74) Patra, N.; Ray, D.; Aswal, V. K.; Ghosh, S. Exploring Physicochemical Interactions of Different Salts with Sodium N-Dodecanoyl Sarcosinate in Aqueous Solution. *ACS Omega* **2018**, *3* (8), 9256–9266. https://doi.org/10.1021/acsomega.8b00718.
- (75) Li, D.; Wagner, N. J. Universal Binding Behavior for Ionic Alkyl Surfactants with Oppositely Charged Polyelectrolytes. *J. Am. Chem. Soc.* **2013**, *135* (46), 17547–17555. https://doi.org/10.1021/ja408587u.
- (76) Olesen, N. E.; Westh, P.; Holm, R. Determination of Thermodynamic Potentials and the Aggregation Number for Micelles with the Mass-Action Model by Isothermal Titration Calorimetry: A Case Study on Bile Salts. *J. Colloid Interface Sci.* **2015**, *453*, 79–89. https://doi.org/https://doi.org/10.1016/j.jcis.2015.03.069.
- (77) Nagarajan, R.; Ruckenstein, E. Theory of Surfactant Self-Assembly: A Predictive Molecular Thermodynamic Approach. *Langmuir* **1991**, *7* (12), 2934–2969.
- (78) Friedowitz, S.; Salehi, A.; Larson, R. G.; Qin, J. Role of Electrostatic Correlations in Polyelectrolyte Charge Association. *J. Chem. Phys.* **2018**, *149* (16), 163335/1-14. https://doi.org/10.1063/1.5034454.
- (79) Wang, Z.-G. Fluctuation in Electrolyte Solutions: The Self Energy. *Phys. Rev. E* **2010**, *81* (2), 21501/1-12. https://doi.org/10.1103/PhysRevE.81.021501.
- (80) Delaney, K. T.; Fredrickson, G. H. Theory of Polyelectrolyte Complexation—Complex Coacervates Are Self-Coacervates. *J. Chem. Phys.* **2017**, *146* (22), 224902/1-14. https://doi.org/10.1063/1.4985568.
- (81) Salehi, A.; Larson, R. G. A Molecular Thermodynamic Model of Complexation in Mixtures of Oppositely Charged Polyelectrolytes with Explicit Account of Charge Association/Dissociation. *Macromolecules* **2016**, *49*

- (24), 9706-9719. https://doi.org/10.1021/acs.macromol.6b01464.
- (82)Ono, Y.; Kawasaki, H.; Annaka, M.; Maeda, H. Effects of Micelle-to-Vesicle Transitions on the Degree of Counterion Binding. J. Colloid Interface Sci. 2005, 287 (2), 685-693. https://doi.org/https://doi.org/10.1016/j.jcis.2005.02.021.
- (83)Klamt, A. Conductor-like Screening Model for Real Solvents: A New Approach to the Quantitative Calculation of Solvation Phenomena. J. Phys. Chem. 1995, 99 (7), 2224–2235. https://doi.org/10.1021/j100007a062.
- (84)Klamt, A.; Jonas, V.; Bürger, T.; Lohrenz, J. C. W. Refinement and Parametrization of COSMO-RS. J. Phys. Chem. A 1998, 102 (26), 5074-5085. https://doi.org/10.1021/jp980017s.
- (85)Liyana-Arachchi, T. P.; Jamadagni, S. N.; Eike, D.; Koenig, P. H.; Siepmann, J. I. Liquid-Liquid Equilibria for Soft-Repulsive Particles: Improved Equation of State and Methodology for Representing Molecules of Different Sizes and Chemistry in Dissipative Particle Dynamics. J. Chem. Phys. 2015, 142 (4), 44902. https://doi.org/10.1063/1.4905918.

TOC:



Anionic surfactant concentration